Development of neuronal connectivity in the central nervous system of *Drosophila melanogaster*

This dissertation is submitted for the degree of Doctor of Philosophy.

Javier Valdes Aleman

University of Cambridge

Robinson College

September 2018

Preface

The work described in this thesis was carried out at the Department of Zoology of the University of Cambridge and the Janelia Research Campus of the Howard Hughes Medical Institute from October 2014 to September 2018.

This dissertation is the result of my own work and includes nothing which is the outcome of work done in collaboration. It is not substantially the same as any that has been submitted or is being concurrently submitted for a degree or diploma or other qualification at the University of Cambridge or any other University or similar institution.

This thesis does not exceed 60,000 words.

Abstract

Our nervous system is made of billions of neurons that process sensory information and control behavior. It is organized into circuits with specifically tuned cell-to-cell connections that are essential for proper function. During development, neurons project to remote locations in search of their synaptic partners. Surrounded by numerous cells along their trajectory and in their target area, these developing neurons ignore most neurons with which they come into contact and connect with very specific partners. The mechanisms by which presynaptic axon terminals and postsynaptic dendrites recognize each other and establish the correct number of connections with the appropriate strength are poorly understood. Sperry's chemoaffinity hypothesis proposes that pre- and postsynaptic partners express specific combinations of molecules that enable them to recognize each other. Alternatively, Peters' rule proposes that presynaptic axons and postsynaptic dendrites use non-partner-derived global positional cues to independently reach their target area, and once there they randomly connect with any available neuron. These connections can then be further refined by additional mechanisms based on synaptic activity.

I use the *Drosophila* embryo and larva, a tractable model system, to test these hypotheses and elucidate the roles of 1) global positional cues, 2) partner-derived cues and 3) synaptic activity in the establishment of selective connections in the developing nerve cord. I altered the position or activity of presynaptic partners and analyzed the effect of these manipulations on number of synapses with postsynaptic partners, strength of functional connections, and behavior controlled by these neurons. For this purpose, I combined developmental live imaging, electron microscopy reconstruction of circuits, functional imaging of neuronal activity, and behavioral experiments in wildtype and experimental animals.

I found that postsynaptic dendrites are able to find, recognize, and connect to their presynaptic partners even when these have been shifted to ectopic locations through the

overexpression of receptors for midline guidance cues. This suggests that neurons use partner-derived cues that allow them to identify and connect to each other. However, while partner-derived cues are sufficient for recognition between specific partners and establishment of connections; without orderly positioning of axon terminals by positional cues and without synaptic activity during embryonic development, the number and strength of functional connections are altered with significant consequences for behavior. Thus, multiple mechanisms including global positional cues, partner-derived cues, and synaptic activity contribute to proper circuit assembly in the developing *Drosophila* nerve cord.

Acknowledgements

I would like to thank my supervisor Marta for letting me work in her lab on such an exciting project, for her intellectual mentorship, for having the patience to teach me, and for her flexibility and trust to allow me to explore and learn in the lab.

During my time in Cambridge, I had the incredible support from Matthias. I would like to thank him for his guidance and for teaching me with great patience. I would also like to thank Greg and all his lab, particularly Seba and Ben, for being so welcoming and friendly with me after I had just arrived at Cambridge. I also want to thank my friends from college Juli, Tom, Stephan and Josh for making my time in Cambridge much more enjoyable.

I have an amazing group of friends at Janelia that have made my time there so amazing. I want to particularly thank Becca, Tam and Elise for those long conversations in the lab and all their support. Without them, working in the lab would not have been the same.

I want to thank my family that has always believed in me and encouraged me this whole time. None of this would have been possible without them. I want to particularly thank my sister Maggie for always being there to listen to me and share advice whenever I needed it.

And finally, but not least, I want to thank Clayton for being amazingly supportive with me. You have been my rock during this big challenge. Thank you for your unconditional support and for putting up with a stressed graduate student!

Contents

Abbreviations and acronyms

AEL	After Egg Laying
CNS	Central Nervous System
EM	Electron Microscopy
GFP	Green Fluorescent Protein
Kir	Inwardly-rectifying potassium channel
mhc	myosin heavy chain
NMJ	Neuro Muscular Junction
Shi^{ts1}	Shibire, temperature-sensitive
tdT	tandem dimer Tomato
TNT	Tetanus Toxin light chain
TrpA1	Transient Receptor Potential cation channel, subfamily A, member 1
UAS	Upstream Activating Sequence
VNC	Ventral Nerve Cord

Chapter 1

Introduction

Formation of neural circuits

Our nervous system is made of billions of neurons that process sensory information and control behavior. It is organized into circuits with multiple neurons forming intricate pathways for optimal information processing. These specifically tuned cell-to-cell connections are essential for proper circuit function. Defects in these connections can lead to major nervous dysfunctions. The mechanisms through which the nervous system achieves such complex and specific connections have been a long-standing focus of study.

Axon guidance along the way to the target area

During development, neurons project to remote locations in search of their synaptic partners. As they navigate the nervous system, neurons travel through the tissue following complex routes that eventually take them to their target location. Developing neurons navigate the nervous system sampling their environment as they contact multiple positional cues (Araújo and Tear, 2003). Neurons are sensitive to these cues in a time-dependent manner, responding to them step-by-step, by steering their direction along their trajectory (Chilton, 2006). These molecules guide neurons to their target location, where they will meet their synaptic partners (Tessier-Lavigne and Goodman, 1996).

Along their developmental paths, neurons establish transient contacts with cells that are not meant to be synaptic partners. These temporary interactions can serve as intermediate targets that allow neurons to break down their long and elaborate trajectories into a series of shorter steps (Chao et al., 2009). Therefore, these interactions occur in a specific spatial location that corresponds to a particular time in development and serves as a decision point so that the developing neuron can steer itself to the next target. These ‘guidepost cells’

enable the developing neurons to follow step-by-step instructions until they reach their final target location. Alternatively, a continuous set of cells can form a scaffold that neurons can recognize and follow along as they keep growing. These pioneering neurons can set the tracks and serve as substrate for later-born neurons following similar trajectories (Jacobs and Goodman, 1989).

Aside from chemical cues, the timing of developmental events (Jefferis et al., 2001) as well as the biophysical properties of the tissue (Koch et al., 2012; Koser et al., 2016) may influence the trajectories to target locations and wiring patterns of developing neurons.

Global positional cues for specifying the target area

Findings in both *Drosophila* and mice have shown that the final location of sensory axon terminals in the developing nerve cord is regulated independently of their partner dendrites (Sürmeli et al., 2011; Zlatic et al., 2003, 2009). In the developing *Drosophila* embryo, the location of sensory axon terminals in the nerve cord is controlled by a system of global positional cues (Araújo and Tear, 2003).

Slit is a positional cue secreted by midline glia which patterns the nerve cord with a concentration gradient decreasing from the midline to the lateral ends (Brose et al., 1999; Kidd et al., 1999). Roundabout (Robo) receptors are expressed by neurons, regulating their proximity to the midline (Kidd et al., 1998a, 1999). Robo receptors bind to Slit and mediate repulsion to it, and therefore repel the neurons that bear them from the midline (Dickson and Gilestro, 2006). Different Robo receptors respond differently to Slit which results in a variation of repulsion degrees, depending on the specific receptor that is expressed (Evans and Bashaw, 2010; Rajagopalan et al., 2000; Simpson et al., 2000a, 2000b). Axons in the medial domain of the nerve cord express Robo, intermediate axons express Robo3 and Robo, while lateral axons express Robo2, Robo3, and Robo. Robo mediates mild repulsion from the midline, Robo3 a moderate repulsion, while Robo2 mediates de strongest repulsion. Therefore, the particular combination of Robo receptors a neuron expresses determines the position it takes in the mediolateral axis. Manipulating the expression levels of Robo receptors is sufficient to shift the locations of sensory axon terminals, independently of their partners.

Silencing the expression of Robo receptors or Slit results in aberrant midline crossing (Long et al., 2004; Simpson et al., 2000b), while their overexpression results in no midline crossing and the collapse of axonal longitudinal tracts (Simpson et al., 2000a).

However, many neurons in the ventral nerve cord (VNC) cross the midline and terminate their axons contralaterally from their cell bodies (Araújo and Tear, 2003). These axons must be attracted to the midline and then repelled from it as they navigate to their target location. Therefore, axons that normally cross the midline commissure lack all three Robo receptors when they go through (Kidd et al., 1998a). Commissureless is a protein found in high concentrations at the midline and reduces midline repulsion by downregulating the expression of Robo (Georgiou and Tear, 2002; Kidd et al., 1998b; Tear et al., 1996). However, Robo expression can be switched back on right after the axons have already crossed the commissure, allowing them to continue their trajectory away from the midline.

Additionally, midline glia secrete another positional cue called Netrin which also forms a concentration gradient in the mediolateral axis, with the highest concentration at the midline (Harris et al., 1996; Kennedy et al., 1994; Mitchell et al., 2009; Serafini et al., 1994). Frazzled is the receptor that binds to Netrin and mediates attraction to it (Keino-Masu et al., 1996; Kolodziej et al., 1996). Frazzled is expressed by commissural axons and allows them to approach the midline. In fact, Frazzled can also bind Netrin and redistribute it in the nervous system, localizing it in an area away from where it was originally expressed (Hotta et al., 2000). Together, Slit and Netrin control midline repulsion and attraction, respectively, in *Drosophila* embryo.

Sensory axon positioning in the dorsoventral axis of the *Drosophila* embryo is patterned by several members of the Semaphorin family (Pasterkamp and Kolodkin, 2003; Zlatic et al., 2009). These secreted and membrane-bound repellents form concentration gradients in the dorsoventral axis. Specific Plexin receptors bind to specific Semaphorins and guide developing axons through repulsive interactions to terminate in the appropriate dorsoventral location, independently of the mediolateral location (Zlatic et al., 2009).

Together, Slit, Netrin, and some Semaphorins function as global positional cues that pattern the *Drosophila* embryo nerve cord and guide the positioning of sensory axon terminals in the mediolateral and dorsoventral axes.

Synaptic specificity theories

Surrounded by numerous cells along their trajectory and in their target area, developing neurons ignore most other neurons with which they come into contact, and connect only with very specific partners. In recent years, detailed high-resolution imaging of the nervous system has allowed the comprehensive reconstruction of neural circuits, revealing striking synaptic specificity (Gerhard et al., 2017; Helmstaedter et al., 2013; Jovanic et al., 2016; Kasthuri et al., 2015; Lee et al., 2016; Ohyama et al., 2015; Schneider-Mizell et al., 2016; Takemura et al., 2013, 2015; White et al., 1986; Zheng et al., 2018). These studies suggest neurons discriminate from the vast collection of other available neurons and connect only with a subset of them.

However, despite significant progress in elucidating mechanisms of axon guidance and axon targeting, much less is known about the mechanisms by which presynaptic axon terminals and their postsynaptic dendrites recognize each other and establish the right number of connections with appropriate strength.

In order for a pair of neurons to establish connections with each other, pre- and postsynaptic elements must occupy the same location in the nervous system for synaptogenesis to happen. In principle, these partners could follow similar global location cues that independently guide them to converge at the same location where they both would randomly form synapses with the neurons around them. This locational restriction might be sufficient to generate connections that are selective enough to establish functional circuits (Li et al., 2007; Roberts et al., 2014). Peters' rule intends to predict synaptic connectivity based on the extent of colocalization of a given pair of neurons (Peters and Feldman, 1976; Rees et al., 2017). This hypothesis implies that connectivity is a result of spatial coincidence and independent of the particular partner cells involved. Additionally, once neurons have made synapses with each other, these connections can be further refined through activity-dependent mechanisms.

Hebb's rule claims that the repetitive and persistent stimulation of a postsynaptic neuron by a presynaptic cell leads to the strengthening of their connections (Brown et al., 2009; Hebb, 1949). In other words, "*neurons that fire together, wire together*". Therefore, randomly generated connections early in development can later be eliminated to maintain only those that are functionally relevant. This way, a common location determined by global positional cues and refinement of connections through activity could lead to the formation of functional circuits (Katz and Shatz, 1996; Leighton and Lohmann, 2016).

The neuromuscular junction (NMJ) of *Drosophila* has been used extensively to study synaptic specificity. There has been progress in understanding the *in vivo* interactions between motoneurons and muscles at the NMJ during development (Kohsaka and Nose, 2009; Vonhoff and Keshishian, 2017a, 2017b; Zito et al., 1999). Motoneuron axons travel a long way from the central nervous system (CNS) to the periphery to target single muscle fibers. Since the muscles are relatively static, the partner searching process is performed mostly by the presynaptic axons. They often form promiscuous synapses with more than one muscle and later refine them by eliminating off-target connections in an activity-dependent manner (Carrillo et al., 2010; Jarecki and Keshishian, 1995; Keshishian et al., 1993, 1994; Menon et al., 2013). Low frequency calcium oscillation in filopodia seem to signal whether a given contact is maintained or removed (Vonhoff and Keshishian, 2017a, 2017b), as similarly observed in vertebrates (Lohmann and Bonhoeffer, 2008; Lohmann et al., 2002). In fact, motoneurons in the embryo respond to various amounts of synaptic input by regulating the size of their dendritic arbor to maintain homeostasis of their overall input (Tripodi et al., 2008). Similar experience-dependent activity regulates the dendritic dynamics, morphology, and synapse numbers of second-order visual neurons in the larva (Sheng et al., 2018; Yuan et al., 2011).

Contrastingly, there are also several reports that claim neuronal activity is not required for circuit formation in *Drosophila*. Silencing motoneurons had no effect on their morphology or their capacity to establish connections in the embryo (Baines et al., 2001). Lack of visual input by depriving the animals of light or through various neuronal activity mutants had no apparent effect on circuit assembly in the visual system (Hiesinger et al., 2006; Scott et al., 2003). Similarly, neuronal activity does not seem to be required for the development of the olfactory system of the embryo or adult (Jefferis et al., 2004; Prieto-Godino et al., 2012).

However, the absence of spontaneous activity can also lead to morphological (Prieto-Godino et al., 2012) and behavioral alterations (Utashiro et al., 2018). Therefore, the role of synaptic activity in circuit assembly is still an open question.

Sperry's chemoaffinity theory is an opposite but prominent hypothesis that suggests pre- and postsynaptic partners express specific combinations of molecules that enable them to recognize each other to establish specific connections (Meyer, 1998; Sperry, 1963). This theory is based on a famous experiment Roger Sperry performed in which he severed the optic nerve of a frog, rotated the eye 180°, and reinserted it (Sperry, 1943). The optic nerve regenerated back into the optic lobe and the animals recovered vision. However, the visual map of the frog was now also rotated. When the animal was presented food below it, it would turn its head up, and vice versa. This suggested neuron encoding visual information from the now ventral (dorsal before manipulation) field of view had innervated the dorsal visual domain in the brain. This proved that the nerves in the eye had kept their original wiring targets regardless of the new rotated position from where they were growing. Sperry stated that *"growing fibers are extremely particular when it comes to establishing synaptic connections, each axon linking only with certain neurons to which it becomes selectively attached by specific chemical affinities"* (Sperry, 1963). This and other similar experiments that Sperry performed were evidence that these neurons were following some kind of wiring specificity instructions to keep their orderly connections.

These results led Sperry to propose his chemoaffinity theory, which claims that there must be particular molecular tags that allow partner neurons to identify and connect to each other (Sperry, 1963). This means neurons would be able to differentiate the correct partner neurons from all irrelevant neurons in the immediate surroundings. Therefore, this hypothesis implies neurons embark on their developmental journey to find a specific set of partner cells that is genetically predefined.

More recent studies have identified several molecules that have been shown to be involved in synaptic specificity (Heiman and Shaham, 2010; Rawson et al., 2017; Shen and Scheiffele, 2010; Tavosanis, 2012; Williams et al., 2010). The visual (Clandinin and Zipursky, 2002; Millard and Pecot, 2018; Nériec and Desplan, 2016) and olfactory (Hong and Luo, 2014; Li et al., 2018)

systems in *Drosophila* have been widely used as models for circuit formation. Their highly organized circuit structure makes them suitable for these types of studies. Some of these molecules promote the formation of synapses between specific neurons through homophilic interactions such as Teneurins in the olfactory system (Hong et al., 2012) or n-Cadherins mediating cartridge formation in the optic lobe (Schwabe et al., 2014), while others inhibit the formation of connections between non-partner neurons and muscles at the NMJ (Inaki et al., 2007). Additionally, the Dscam protein family has a particularly large splicing-derived variability, and has been found to impart molecular identity to neurons and mediate homophobic repulsion between neurites of the same neurons (self-avoidance) (Chen et al., 2006; Hughes et al., 2007; Matthews et al., 2007; Millard et al., 2010; Schmucker et al., 2000; Soba et al., 2007; Zipursky and Grueber, 2013). Highly structured connectivity patterns like the ones in the olfactory and visual circuits are not necessarily prevalent across the nervous system, suggesting synaptic specificity might be a much more challenging task in other less compartmentalized circuits.

Nevertheless, the extent to which presynaptic axons and postsynaptic dendrites specifically seek out each other during embryonic development, or the extent to which they simply seek out a common target area and connect to whichever neurons are there, remains an open question.

The roles of global positioning guidance cues, partner-specific selectivity cues, and activity-dependent synaptic refinement are not necessarily mutually exclusive. However, the extent to which their concerted interplay influences the formation of a fully functional circuit is unclear.

Overcoming major obstacles to progress in the field

Elucidating the mechanisms by which selective connections are established requires the ability to independently manipulate gene expression and synaptic activity in specific neurons, while monitoring the effects on structural and functional connections with their specific partners and on behavior. However, in most systems, synaptic-resolution connectivity maps are not available, and the ability to selectively manipulate specific circuit elements while

monitoring the effects of these manipulations on synapse numbers, functional connections, and behavior is not possible.

I have overcome these obstacles by using the tractable *Drosophila* embryo and larva as a model system that offers the following advantages. First, the *Drosophila* larva has a compact nervous system that can be rapidly imaged with modern-day electron microscopy (EM) (Berck et al., 2016; Eichler et al., 2017; Gerhard et al., 2017; Jovanic et al., 2016; Ohyama et al., 2015; Schlegel et al., 2016; Schneider-Mizell et al., 2016), and circuits can be reconstructed from such image volumes with synaptic resolution (Briggman and Bock, 2012; Helmstaedter, 2013; Helmstaedter et al., 2011). Furthermore, it is possible to rapidly image with EM and reconstruct multiple nervous systems, from both wildtype and experimental animals. Second, exquisite genetic tools have been developed for selective and independent targeting of individual circuit elements (Jenett et al., 2012; Pfeiffer et al., 2008, 2010; del Valle Rodríguez et al., 2012; Venken et al., 2011). With these tools it is possible to manipulate gene expression and activity in specific presynaptic partners, while monitoring the activity or morphology of postsynaptic partners. Third, highly sensitive quantitative methods have been developed for monitoring behavioral responses to specific stimuli and comparing behavior of wildtype and experimental animals (Kabra et al., 2013; Ohyama et al., 2013; Vogelstein et al., 2014).

I have used this system to test 1) the role of global positional cues in selective synaptogenesis; 2) whether pre- and postsynaptic neurons specifically attract and recognize each other; and 3) the role of activity in refining connections. I combined electron microscopy reconstruction of circuits, functional imaging of neuronal activity, and behavioral experiments in wildtype and experimental animals. I altered receptors for global positional cues, or activity in presynaptic partners and analyzed the effect of these manipulations on synapse numbers, functional connections, and behavior controlled by this circuit.

A mechanosensory circuit in *Drosophila* larva as a model for studying the establishment of selective connections

I chose the mechanosensory circuit of *Drosophila* larva as a model system for studying selective synaptogenesis for the following reasons. First, the morphology and function of mechanosensory chordotonal neurons has been well characterized (Kavlie and Albert, 2013; Merritt and Whitington, 1995; Ohyama et al., 2013; Schrader and Merritt, 2000). Second, the postsynaptic partners of all mechanosensory neurons in the abdominal segments of the larval nerve cord have been identified using EM reconstruction, and the relative numbers of connections was found to be stereotyped for each pair of neurons (Jovanic et al., 2016; Ohyama et al., 2015). And third, the behavioral roles of these sensory neurons, and several interneurons in this circuit have been characterized (Jovanic et al., 2016; Ohyama et al., 2013, 2015).

The mechanosensory Chordotonal neurons

The chordotonal organs are discrete and organized groups of cells across the external insect body involved in mechanosensation (Kavlie and Albert, 2013). These organs contain one or more units called scolopidia that are composed of different types of cells: one or more sensory neurons with ciliated dendrites, the cap cell that connects the neuron to the outer cuticle, the scolopale cell that surrounds the distal dendrite, and the ligament cell that anchors the neuron to the inner cuticle (Kernan, 2007).

The chordotonal sensory neurons (or Chordotonals for brevity) function as stretch receptors that detect mechanical stimuli and can act as proprioceptors (Caldwell et al., 2003) or exteroceptors. For example, air vibration generated by sound can pull on the scolopidium's cap and stretch the neuron's cilium, activating mechanically-gated ion channels. However, the chordotonal organs can transduce different stimuli and convey different meanings, depending on their location in the body and the tissue they are attached to (Kamikouchi et al., 2009; Kavlie and Albert, 2013; Shanbhag et al., 1992).

In *Drosophila* embryo and larva, each chordotonal organ on the body wall can contain one or more sensory neurons. Eight Chordotonal neurons are present in either side of each abdominal segment: five (lch5-1 through lch5-5) in the lateral pentascolopidial chordotonal organ, one (v'ch1) in the lateral monoscolopidial chordotonal organ, and two (vchA and vchB) in the ventral chordotonal organ (Hartenstein, 1993; Merritt and Whitington, 1995; Schrader and Merritt, 2000). The chordotonal organs repeat with the same organization in every abdominal segment. A total of 16 Chordotonal axons per abdominal segment project from the periphery to the CNS, entering the VNC at their respective segment. The lch5 neurons enter through the intersegmental nerves, while v'ch1, vchA and vchB enter through the segmental nerves. All Chordotonal axons from the same hemisegment arborize in close proximity of each other. They span mostly along the anterior-posterior axis across one or two segments with stereotypic and identifiable morphologies (Merritt and Whitington, 1995; Zlatic et al., 2003).

The mechanosensory circuit of *Drosophila* larva

EM reconstruction of larval neurons has unveiled the complexity and magnitude of connections in neural circuits (Berck et al., 2016; Eichler et al., 2017; Jovanic et al., 2016; Ohyama et al., 2015; Schlegel et al., 2016). *Drosophila* larva neurons seem to form hundreds of synapses with tens of partner cells. However, within the overwhelming complexity of circuits, neurons make reproducible connections to form functional circuits.

Recent work explored in detail the circuits downstream of Chordotonal neurons in *Drosophila* larva using EM reconstruction, functional imaging, and behavioral assays (Jovanic et al., 2016; Ohyama et al., 2015). This revealed that the Chordotonal neurons connect to several excitatory and inhibitory local interneurons. Ladder, Griddle and Drunken are groups of inhibitory neurons immediately downstream of the Chordotonals that form levels of lateral, feedforward, and feedback inhibitory connections. This results in a series of disinhibitory interactions that regulate the selection of mechanically-evoked behavior in the larva (Jovanic et al., 2016). These inhibitory neurons connect to each other and to other excitatory neurons directly downstream of Chordotonals, such as long-range projection neurons, and local Basin interneurons.

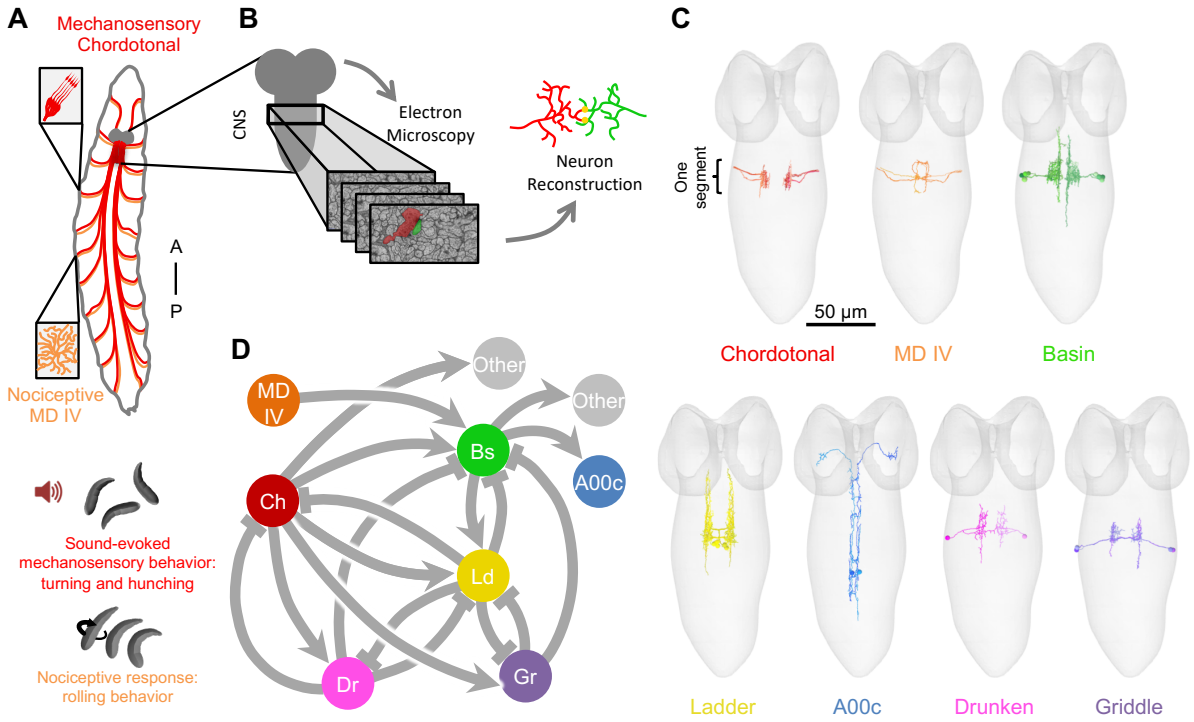

Figure 1. A mechanosensory circuit in *Drosophila* larva revealed by electron microscopy reconstruction.

A) Schematic of the mechanosensory Chordotonal neurons (red) and the nociceptive multidendritic class IV (MD IV) neurons (orange) spanning the larval body wall and projecting their axons into the CNS. Insets illustrate the morphology of these neurons at the body wall. Vibration generated by sound activates the mechanosensory neurons and elicits a stereotypic behavior consisting of turns and hunches. While activation of MD IV elicits a rolling escape response.

B) Electron micrographs of thin sections of the CNS allow for high-resolution reconstruction of neurons revealing fine morphology and connectivity.

C) Skeletonized reconstructions of neurons involved in the mechanosensory circuit generated from EM. Neurons from one abdominal segment (segment A4 for A00c and A1 for all other neurons) of a first instar larva are shown inside the outline of the CNS (gray). Only neurons originating within one abdominal segment are shown for illustration purposes; however, these neurons repeat across multiple segments. These images show 16 individual Chordotonal axons, 6 MD IV axons, 8 Basins, 6 Ladders, 2 A00c, 2 Drunkens and 4 Griddles.

D) Connectivity diagram of key neurons of the mechanosensory circuit revealed by EM reconstruction. The Chordotonal neurons (red) are direct upstream partners of three groups of inhibitory interneurons: Griddles (purple), Drunkens (pink) and Ladders (yellow). The excitatory Basins cells (green) are a point of multisensory convergence, being directly downstream of the mechanosensory Chordotonals and the nociceptive MD IV neurons (orange). A00c neurons (purple) are excitatory ascending neurons that collect Basin input along the nerve cord and project their axons to the brain. Other neurons downstream of the mechanosensory circuit represent an alternative pathway (gray) not explored in this study. This diagram includes strong synaptic partners that are key for this study, but it does not include all partners. Each circle represents a group of neurons, as opposed to individual neurons. The arrows indicate the direction of the connections: regular arrows represent excitatory connections, and flathead arrows represent inhibitory ones.

Basins neurons are multisensory integration points, directly downstream of both the mechanosensory Chordotonal neurons and the nociceptive multidendritic class IV (MD IV) neurons. The MD IV neurons are sensory neurons that respond to noxious stimuli like harsh touch and heat; and can trigger escape behavioral responses in the larva (Hwang et al., 2007; Robertson et al., 2013; Tracey et al., 2003). This sensory convergence at the Basin level enhances escape behavior selection based on the specific combination of multisensory input (Ohyama et al., 2015). Additionally, all the neurons downstream of the Basin interneurons have also been reconstructed using EM (Ohyama et al., 2015). These included A00c ascending excitatory neurons that collect Basin input along the VNC and project their axons to the brain. These studies have revealed the circuit involved in mechanosensation through the Chordotonal neurons, and the neurons that are shared with the nociceptive circuit, which all together incorporate the sensory, local, and ascending interneurons that I focus on for this thesis (see **Figure 1**).

Functional and behavioral roles of the mechanosensory circuit

Electrophysiological and behavioral studies have shown that Chordotonal neurons in the larva respond to sound-generated vibration (Ohyama et al., 2013, 2015; Wu et al., 2011) and to air puff (Jovanic et al., 2016). Larvae respond to vibration with stereotypic behavior by bending

their bodies, hunching, or both. These behaviors can also be triggered by genetically activating Chordotonals. Conversely, silencing Chordotonals leads to a significantly reduced behavioral response to mechanical stimuli (Jovanic et al., 2016; Ohyama et al., 2013, 2015).

The MD IV neurons are involved in the escape response of the larva by triggering bending, fast crawl, and rolling behaviors. In nature, larvae roll as an escape mechanism when they are under attack by a parasitoid wasp, their natural predator (Hwang et al., 2007; Robertson et al., 2013). In fact, the genetic activation of Basin neurons, direct downstream partners of MD IV, also evokes vigorous rolling behavior (Ohyama et al., 2015). However, Basins trigger rolling with a higher probability than MD IV. Conversely, the activation of Chordotonals (upstream of Basins) never triggers rolling. Interestingly, when Chordotonals and MD IV are both activated simultaneously, they synergistically evoke an even stronger rolling response (Ohyama et al., 2015). This enhanced behavioral response in mediated by Basins, the common downstream partner of these two sensory modalities.

In the following chapters I describe experiments in which I used this model circuit to explore the effects of manipulating the position of Chordotonal terminals or their activity on 1) the number of their connections with excitatory and inhibitory interneurons, 2) on the strengths of functional connections with their downstream partners, 3) and on the animal's response to vibration and noxious stimuli.

Chapter 2

Materials and methods

Fly stocks

All animals used in this study are of the *Drosophila melanogaster* species and were kept on fly food at 25 °C unless otherwise specified. The fly food composition is as follows: molasses 5.1% v/v, dry yeast 2.04% m/v, corn meal 8.45% m/v, agar 0.75% m/v, Tegosept 0.2% v/v, and propionic acid 0.5 % v/v. Animals for optogenetic experiments were kept in the dark on fly food supplemented with all-trans-retinal (Cat. #R240000, Toronto Research Chemicals) to a concentration of 0.5 mM.

All throughout this document, abbreviated names of the fly strains have been used for simplicity. See **Table 1** for full genotypes and other details of all the fly lines used in this study. Different driver lines were used to restrict the expression of a given transgene to the neurons of interest. The GAL4/UAS, LexA/LexAop, and QF/QUAS binary expression systems (del Valle Rodríguez et al., 2012) were used interchangeably. The specific expression system used for each experiment is stated where appropriate.

The *R72F11* driver was used for transgene expression in Basin cells (Ohyama et al., 2015), *iav* or *R61D08* for Chordotonal mechanosensory neurons (Kwon et al., 2010; Ohyama et al., 2015), *ppk* for multidendritic class IV neurons (Ainsley et al., 2003), and *R71A10* for A00c neurons (Ohyama et al., 2015). The *w;; attP2* line (fly line 32, **Table 1**) has an empty insertion site with no driver and was used as control for some experiments (where indicated).

Live imaging

For live imaging experiments, fly stocks were generated to label Basin cells with myristoylated GFP using the *72F11-LexA* driver, and the Chordotonal sensory neurons with myristoylated tdTomato using the *iav-GAL4* driver. These animals contained a mutation in the myosin heavy

chain (*mhc[1]*) that disables muscle contraction in homozygous mutants in order to prevent interruptions during the imaging process (Mogami and Hotta, 1981; O'Donnell and Bernstein, 1988; Vonhoff and Keshishian, 2017b). This mutation was kept over the balancer CyO to establish viable stocks. When possible, CyO labelled with dfd-GMR Yellow fluorescent protein (DGY) (Le et al., 2006) was used to facilitate the selection of homozygous embryos. For the live imaging of Basins only, the following line was used: *w; R72F11-LexA, LexAop-GFP, mhc[1]/CyO, DGY; iav-GAL4, UAS-tdT* (fly line 1, **Table 1**). For simultaneous live imaging of Basins and Chordotonals, the following line was used: *w; R72F11-LexAp65 in JK22C, 13XLexAop2-IVS-myr::GFP in su(Hw)attP5, mhc[1]/CyO, DGY; iav-GAL4, UAS-IVS-myr::tdTomato in attP2* (fly line 2, **Table 1**).

Eggs were collected for one hour at 25 °C on agar plates with yeast paste. After collection, the eggs were incubated at 25 °C for 13 hours. Then the eggs were treated with a 1:1 mixture of water and commercial bleach for five minutes or until the chorion was fully removed. The resulting mixture was passed through a sieve to recover the dechorionated eggs. These were rinsed with distilled water to remove bleach and transferred into a Petri dish. Single embryos were carefully picked under a dissection microscope and placed ventral side up on an oxygen-permeable teflon membrane (Lumox). Such membrane was stretched on a custom-made mount that can hold liquid and fits the microscope stage. Multiple embryos were aligned in a row and fully covered with room temperature distilled water. This was done not more than 10 minutes after the embryos were dechorionated to prevent dehydration.

The imaging setup consisted of a Yokogawa CSU-22 spinning disk confocal field scanner mounted on an Olympus BX51 WI fixed-stage upright compound microscope, with an Evolve EMCCD camera (Photometrics) and a LUMPlanFl 60X/0.9 NA (Olympus) water dipping objective. The excitation wavelengths for imaging GFP and tdT were 488 nm and 561 nm, respectively. 50 μm Z-stacks with a 1 μm step size and 218 nm/pixel resolution were acquired in two imaging channels every time point for each embryo. Multiple embryos were imaged one after the other continuously for at least 12 hours. The time point frequency varied from 1 to 5 min depending on the number of embryos imaged simultaneously in each session. The center of the stack in the Z axis was roughly located at the center of the developing ventral nerve cord at the beginning of the imaging session. The imaging range in the Z axis was

manually readjusted during the session if needed to ensure coverage of the neurons of interest. The images were acquired with the control of MetaMorph software (Molecular devices).

Image processing for live imaging data

Standard image processing was performed using Fiji (Rueden et al., 2017; Schindelin et al., 2012). Briefly, the imaging stacks were cropped to remove Z sections that did not contain the neurons of interest. The images were denoised using nd-safir (Boulanger et al., 2010). Z-projections were generated, and the imaging channels were merged to create 2D time-lapse videos of the developing neurons in two colors. Bleach correction (Fiji) was used to adjust for the increasing brightness of the neurons through time. Ilastik (Sommer et al., 2011) was used for pixel classification to generate the segmented images. Different trained pixel classification parameters were used for each imaging channel.

Calcium imaging with GCaMP

Calcium responses were imaged as GCaMP6s (Chen et al., 2013) fluorescence fluctuations in the neurons of interest (Basin or A00c). CsChrimson was expressed in presynaptic neurons (Chordotonal or MD IV) for optogenetic activation (Klapoetke et al., 2014). GCaMP signals were recorded in dissected central nervous systems in a saline solution (135 mM NaCl, 5 mM KCl, 2 mM $CaCl_2 \cdot 2H_2O$, 4 mM $MgCl_2 \cdot 6H_2O$, 5 mM TES, 36 mM Sucrose, pH 7.15) and adhered by the ventral side to a cover glass coated with poly-L-lysine (SIGMA, P1524) on a small Sylgard (Dow Corning) plate.

The calcium imaging experiments were performed using a 3i VIVO Multiphoton upright microscope (Intelligent Imaging Innovations). The Chordotonal neurons were photo-stimulated using a 1040 nm laser (1040-3 femtoTrain, Spectra-Physics) coupled to a 2-photon Phasor (Intelligent Imaging Innovations) to generate a holographic pattern to restrict the activation area. GCaMP responses were recorded using an imaging laser tuned to 925 nm (Insight DS+ Dual, Spectra-Physics) and an Apo LWD 25x/1.10W objective (Nikon).

For the reversible silencing of Chordotonal neurons with Shibire^{ts1} (Chen et al., 1991) and recording of Basin responses the *w; R61D08-LexA; R72F11-GAL4* line (fly line 5, **Table 1**) was crossed to: *w; LexAop-Shi; UAS-GCaMP6s, LexAop-CsChrimson* (fly line 7, **Table 1**) for experimental animals, or to *w;; UAS-GCaMP6s, LexAop-CsChrimson* (fly line 6, **Table 1**) for control. Embryos were collected on retinal food for two hours at 25 °C and then incubated in the dark at 31 °C for 24 hours, and for another day at 18 °C until testing. For the activation of Chordotonal neurons and recording of Basin responses, the stimulation protocol consisted of an initial 30 s resting period, a 100 ms stimulation event, and a final 30 s resting period. A photo-stimulation region of 26.3 μm x 11.9 μm was delimited to contain the Chordotonal axon terminals within one abdominal hemisegment, approximately. The stimulation power value measured at the objective end with a power meter (PM100D Thorlabs) was 34.2 mW. This protocol was executed in three different abdominal hemisegments per sample. Any two stimulated ipsilateral hemisegments were separated by at least one unstimulated hemisegment as a precaution in case of unintended leaky stimulation of the adjacent hemisegment. GCaMP responses were imaged at the Basin axons on a single Z plane at 6.61 frames/s.

For the activation of Chordotonal neurons and imaging of A00c calcium responses, the *w; R61D08-LexA; R71A10-GAL4* (fly line 8, **Table 1**) line was crossed to: *w; LexAop-Shi; UAS-GCaMP6s, LexAop-CsChrimson* (fly line 7, **Table 1**) for experimental animals, or to *w;; UAS-GCaMP6s, LexAop-CsChrimson* (fly line 6, **Table 1**) for control. A photo-stimulation region of 16.2 μm x 56.9 μm was set to cover the Chordotonal axons in the most anterior thoracic hemisegments. The protocol consisted an initial resting period of 30 s, a stimulation event of 200 ms and 323 mW, and a final resting period of 30 s. This protocol was implemented twice per sample, stimulating Chordotonal axons on either side of the nerve cord, one at a time. A00c calcium responses were recorded at their axons in the corresponding side of the brain at 8.79 frames/s.

For the experiments where the Chordotonal neurons were silenced with tetanus toxin (TNT) (Sweeney et al., 1995) and the MD IV neurons were optogenetically activated, the *w; R61D08-LexA; R72F11-GAL4, ppk-QF2* (fly line 11, **Table 1**) line was crossed to: *w, QUAS-CsChrimson;*

LexAop-TNT; UAS-GCaMP6s (fly line 9, **Table 1**) for experimental animals, or to *w, QUAS-CsChrimson;; UAS-GCaMP6s* (fly line 10, **Table 1**) for control animals. Eggs were collected on retinal food and incubated in the dark at 25°C for four days. The dissected samples were left in the dark for at least two minutes immediately before initiating the imaging session. All the MD IV axons were photo-stimulated with a 625 nm LED mounted on the microscope stage to illuminate the entire sample with 170 $\mu W/cm^2$. The stimulation protocol consisted of an initial 30 s resting period, four 1 s stimulation events of the same intensity, each followed by a 30 s resting period. This protocol was executed once per sample. All other imaging details are as stated above.

Image analysis of calcium imaging data

The GCaMP image data were processed using custom macros in Fiji (Schindelin et al., 2012) and analyzed using custom code written in R (R Core Team, 2015). Briefly, a region of interest (ROI) was manually defined to include the corresponding GCaMP-expressing axons. The average pixel value inside such ROI was measured with Fiji across all time points for each sample. All fluorescence values were reported relative to a fluorescence baseline (F_0) defined as the median pixel value of the corresponding ROI during the entire imaging experiment. $\Delta F/F_0$ was calculated as $\Delta F/F_0 = (F_t - F_0)/F_0$, where F_t is the mean fluorescence value of the ROI at a given time point. The relative maximum $\Delta F/F_0$ was defined as the maximum $\Delta F/F_0$ value in a 4.5 s time window immediately after stimulation offset from which the baseline (mean $\Delta F/F_0$ of the 3 s preceding stimulation onset) was subtracted. Those individual trials in which there were no responses were discarded. A trial with no response was defined as that where the mean $\Delta F/F_0$ in the 4.5 s following stimulation was within ± 1.5 (for Chordotonal activation) or ± 0.5 (for MD IV activation) standard deviations of the baseline (3 s preceding stimulation). Individual imaging trials were averaged by animal. The calcium imaging data were plotted using the ggplot2 (Wickham, 2009) package in R.

Behavioral assays

All the behavioral apparatuses used in this study have been described previously (Ohyama et al., 2013, 2015) and will only be explained briefly. The rigs had some common core components and differed mostly in the hardware to deliver different types of stimuli. Generally, all consisted of a temperature-controlled enclosure with a high-resolution camera on top, an array of infrared (850 nm) LEDs for illumination, a computer for data acquisition and storage, and the respective hardware modules to deliver and control different stimuli.

For thermogenetic activation, the neurons of interest expressed the heat-activated cation channel TrpA1 (Hamada et al., 2008; Kang et al., 2012). For these experiments, eggs were collected on food plates for 6-8 hours and incubated at 18 °C for 8 days, unless otherwise stated. The animals were placed on a thin layer of 4% charcoal agar on top of an aluminum plate. This was placed on a Peltier module to control temperature to the desired value. The standard thermogenetic activation protocol consisted of 30 s at 20 °C, followed by a ramping-up period of 40 s to reach 35 °C, 50 s at 35 °C, and a final ramping-down period of 60 s to reach 20 °C. Whenever optogenetic activation was paired with a thermal stimulus, red (630 nm) LEDs were used with a power density of 490 $\mu W/cm^2$ onto the center of the plate.

For vibration experiments, eggs were collected on food plates for 6-8 hours and incubated at 25 °C for four days, unless otherwise stated. The mechanical stimulus was delivered as vibration using a speaker located to the side of a 4% agar plate holding the animals. Tones were played at 1000 Hz, with a measured volume (Extech, 407730) of 122 dB. The protocol consisted of 30 s of no sound, 30 s tone at 1000 Hz, and 30 s of no sound.

For optogenetic activation, animals carried the CsChrimson transgene (Klapoetke et al., 2014) in the neurons of interest. Eggs were collected on retinal food for 6-8 hours and incubated in the dark at 25 °C for four days, unless otherwise specified. When photo-activation was the only stimulus, larvae were placed on a 4% agar plate on top of an array of red (630 nm) LEDs with power density of 638 $\mu W/cm^2$ through the plate. The activation protocol consisted of 30 s of the LEDs being off, 15 s on, 30 s off, 15 s on, and 30 s off.

For each behavioral experiment, a total of roughly 400-500 animals were tested across multiple trials. For experiments performed on a thermal plate, each trial included approximately 20 animals. All other experimental trials included approximately 50 animals each. The number of animals from experiments that included young (before 3rd instar) larvae is much lower due to technical difficulties of handling and tracking smaller animals. Many animal traces are discarded throughout the subsequent analysis pipeline. The resulting number of animals used for statistical analysis varies across experiments and depends on the nature of the behavior evoked, stimulus and size of behavioral plate.

Stimulus control, object detection, and feature extraction were performed by the Multi Worm Tracker and SALAM-LARA (http://sourceforge.net/projects/salam-hhmi) software as previously described (Denisov et al., 2013; Ohyama et al., 2013).

Electron microscopy reconstruction

Four electron microscopy volumes were used in this study. They comprise a whole or partial central nervous system of first instar *Drosophila* larvae. Two of these are control volumes of a *w1118* genotype and have been previously reported (Ohyama et al., 2015). The neurons from the two control volumes were previously reconstructed by members and collaborators of the Cardona lab (Janelia Research Campus, HHMI). The two remaining EM volumes were acquired for this study using the same protocol reported for the control volumes (Ohyama et al., 2015). They have an image resolution of 3.8 nm by 3.8 nm by 40 nm in x, y and z, respectively. These volumes include a 1.5-segment fraction of the central nervous system (A2 and A3 segments) of first instar larvae. The genotypes for these volumes are: 1) *w;; iav-GAL4/UAS-FraRobo* 2) *w; UAS-TNT/+; iav-GAL4/+*. The neurons were reconstructed using CATMAID (Saalfeld et al., 2009) to obtain the skeletonized structure and connectivity of the cells of interest. All the connectivity data were generated in CATMAID and processed in R.

Statistical analysis

Statistical analysis was performed using R. The calcium responses between control and experimental animals were compared using the single-sided Wilcoxon rank-sum test.

For the behavioral assays, the probability of a behavior occurring was calculated as the proportion of animals that performed the specified behavior at least once during the 15 s (for optogenetic activation or vibration stimulus) or 40 s (for thermogenetic activation) immediately after stimulus onset across all trials. The analysis time window for thermogenetic activation is longer due to its slower activation resulting from temperature ramping. Therefore, the stimulus onset for thermogenetic activation experiments was defined as the moment the thermal plate reached 35 °C. Only those animals that were detected for at least 95% of the analyzed time window and did not contacted another animal during this period were included in the analysis. The behavior probabilities were compared using a chi-square test for proportions. Behavior durations were calculated for the time windows mentioned above and compared using a double-sided t-test.

Electron microscopy connectivity data were compared using a chi-square test for proportions.

In all figures, * represents p-value ≤ 0.05, ** represents p-value ≤ 0.01, and *** represents p-value ≤ 0.001.

Table 1. Fly lines used in this study

Fly line number	Genotype	Source	Figure
1	*w; R72F11-LexAp65 in JK22C, 13XLexAop2-IVS-myr::GFP in su(Hw)attP5, mhc[1]/CyO, DGY*	This study. Derived from stocks 21, 24, 34, 36	3.1
2	*w; R72F11-LexAp65 in JK22C, 13XLexAop2-IVS-myr::GFP in su(Hw)attP5, mhc[1]/CyO, DGY; iav-GAL4, UAS-IVS-myr::tdTomato in attP2*	This study. Derived from stocks 1, 3	3.2, 3.3A-C
3	*w;; iav-GAL4, UAS-IVS-myr::tdTomato in attP2*	This study. Derived from stocks 19, 25	4.5E-E’
4	*w;; iav-GAL4, UAS-IVS-myr::tdTomato in attP2, UAS-FraRobo*	This study. Derived from stocks 3, 26	4.5E-E’
5	*w; R61D08-LexAp65 in JK22C; R72F11-GAL4 in attP2*	This study. Derived from stocks 17, 16	5.1E
6	*w;; 20xUAS-IVS-GCaMP6s 15.641 in attP2, 13XLexAop2-CsChrimson-tdTomato in VK00005*	Gift from Vivek Jayaraman (JRC) Derived from FlyStore #3021720	5.1E, F
7	*w; 13XLexAop2-IVS-Syn21-Shibire-ts1-p10 in su(Hw)attP5; 20xUAS-IVS-GCaMP6s 15.641 in attP2, 13XLexAop2-CsChrimson-tdTomato in VK00005*	This study. Derived from stocks 27, 6	5.1E, F
8	*w; R61D08-LexAp65 in JK22C; R71A10-GAL4 in attP2*	This study.	5.1F

		Derived from stocks 22, 18	
9	*w, QUAS-syn21-CsChrimson tdTomato_tr p10 in attP18; pSW922[260b] (LexAop-TNT); 20xUAS-IVS-GCaMP6s 15.641 in attP2*	This study. Derived from stocks 10, 29	5.2B
10	w-, QUAS-syn21-CsChrimson tdTomato_tr p10 in attP18;; 20xUAS-IVS-GCaMP6s 15.641 in attP2	This study. Derived from stocks 28, 30	5.2B
11	w; R61D08-LexAp65 in JK22C; R72F11-GAL4 in attP2, ppk-QF2	22, 16, 23	5.2B
12	w; ppk-LexA in attP40; pJFRC97-20XUAS-IVS-GCamp3-p10 in attP2, pJFRC26-13XLexAop2-IVS-dTrpA1-WPRE in VK00005	Zlatic lab (JRC) FlyStore #3018476	5.2C-C’
13	w; iav-GAL4, UAS-TNT-E	This study. Derived from stocks 20, 35	5.2C-C’
14	w; 13XLexAop2-CsChrimson-tdTomato in attP40/CyO, tb, RFP; ppk-LexA in attP2, 20XUAS-TTS-Shibire-ts1-p10 in VK00005/TM6B	Zlatic lab (JRC) FlyStore #3019095	5.2E-E’
15	w; ppk-LexA in attP40; LexAop-TrpA in VK00005, UAS-Kir 2.1/CyO::TM6b	Zlatic lab (JRC) FlyStore #3005544	5.2D-D’
16	w;; R72F11-GAL4 in attP2	Bloomington stock no. 39786 (Pfeiffer et al., 2008)	
17	w;; R61D08-GAL4 in attP2	Bloomington stock no. 39272 (Pfeiffer et al., 2008)	5.1G-H’, 5.2D-D’, 5.2E-E’
18	w;; R71A10-GAL4 in attP2	Bloomington stock no. 39562 (Pfeiffer et al., 2008)	
19	w;; iav-GAL4	Bloomington stock no. 52273	4.2B, D, 4.3, 4.4B, D,

			4.5A-D, 5.1A-D', 5.2A
20	w; iav-GAL4 in VK00014	Zlatic lab (JRC) Derived from FlyStore #1145583	
21	w; R72F11-LexAp65 in JK22C	Gift from Gerry Rubin (Pfeiffer et al., 2010)	
22	w; R61D08-LexAp65 in JK22C	Gift from Gerry Rubin (Pfeiffer et al., 2010)	
23	w;; ppk-QF2	Derived from Bloomington stock no. 66475	
24	w; 13XLexAop2-IVS-myr::GFP in su(Hw)attP5	Gift from Gerry Rubin FlyStore #1116803	
25	w;; UAS-IVS-myr::tdTomato in attP2	Gift from Gerry Rubin FlyStore #1115544	
26	w;; UAS-FraRobo	(Bashaw and Goodman, 1999)	4.2B, D, 4.3, 4.4B, D, 4.5A-D
27	w; 13XLexAop2-IVS-Syn21-Shibire-ts1-p10 in su(Hw)attP5	Gift from Gerry Rubin FlyStore #3005550	
28	w-, QUAS-syn21-CsChrimson tdTomato_tr p10 in attP18	Zlatic lab (JRC) FlyStore #3028614	

29	w; pSW922[260b] (LexAop-TNT)/CyO	Gift from Barry Dickson (JRC) FlyStore #3014983	
30	w;+; 20xUAS-IVS-GCaMP6s 15.641 in attP2	Gift from Vivek Jayaraman (JRC) FlyStore #3013653	
31	w+;; UAS-Shibire-ts1	FlyCore shared resources FlyStore #1101351	5.1G-H’
32	w;; attP2	FlyCore shared resources FlyStore #1500062	5.1G-H’, 5.2D-D’, 5.2E-E’
33	w; mhc[1]/CyO	Gift from Nick Brown	
34	w; UAS-TNT-E	FlyCore shared resources FlyStore # 1101356	5.1A-D’, E, 5.2A, 5.2C-C’
35	w; (CyO, DGY; TM6B, DGY)/apx	Derived from Bloomington stock no. 8623 and 8704 (Le et al., 2006)	

Chapter 3

Visualizing dendritic and axonal exploration during development

Introduction

The extent to which presynaptic axons and postsynaptic dendrites specifically seek out each other during embryonic development, or the extent to which they simply seek out a target area and connect to any available neurons there, remains an open question. In the *Drosophila* nerve cord, presynaptic somatosensory axons were shown to use positional guidance cues to select where to terminate, branch, and establish synaptic connections (Zlatic et al., 2003, 2009). However, whether their partner dendrites explore their environment seeking out specific presynaptic axons, or whether they connect with whichever axon terminal they contact is unknown. Addressing these questions requires visualizing the developing axons and dendrites of partner neurons when they first start growing to their target area and contacting each other. Therefore, for this chapter I investigated the earliest contacts between the Chordotonal and Basin neurons in the VNC.

I performed live imaging in the intact embryo and observed the mechanistic interactions between these partner neurons during development (see **Figure 3.1A**). I generated transgenic fly lines to simultaneously label Chordotonal and Basin neurons with two different myristoylated fluorescent reporters in the same animal. These lines included a mutation in the myosin heavy chain (*mhc*) gene (Mogami and Hotta, 1981; O'Donnell and Bernstein, 1988) to prevent muscle contraction and allow the acquisition of smooth time lapse movies (Vonhoff and Keshishian, 2017b). The samples were imaged at multiple time points (every 1-5 min depending on the sample) with a spinning-disk confocal microscope. I followed the development of Chordotonal and Basin neurons from the earliest moment of fluorophore expression until the end of the embryonic stage (≥ 12-hour long imaging session). I discovered the dynamic development of the axons and dendrites of these cells and the interaction between them in the VNC.

Results

Embryonic development of Basin neurons

Under the *R72F11-LexA* driver, a few Basin cells start expressing detectable levels of GFP around 13 hours after egg laying (AEL), which marks the beginning of the imaging session (see **Figure 3.1B**). The rest of the cells are detected sporadically shortly after. At this early stage, Basins have an immature morphology consisting of the cell body laying laterally and a primary branch extending from it toward the midline. Approximately in the middle of this primary branch there is a swelling which will become the site for dendrite initiation. The leading end at the most medial side of the cell is the growth cone of the developing axon.

When the Basin axon reaches the appropriate anterolateral tract (perpendicular to it), it proceeds to split into two long projections in the same dorsoventral plane, one end extending anteriorly and the other posteriorly (see **Figure 3.1B**). Both ends of the axon keep extending as they discretely explore their vicinity. Eventually, the axon extends long enough and overlaps with the labeled axons of the neighboring Basins from the adjacent segments. This bundle of axons keeps getting thicker as more Basin neurons are labeled or additional axons from Basins in more distant segments join. Even though it is not possible to distinguish individual axons at this point, we know from the EM reconstructions that Basin axons normally span across one to two segments on either side (Ohyama et al., 2015).

Shortly after the Basin axon splits and starts extending in the anteroposterior axis, the dendrites start developing (see **Figure 3.1B**). Short exploratory filopodia start projecting in all directions from the initiation point at the primary branch, tending to project more medially. These filopodia are short-lived and normally retract within a few minutes. The number and length of dendritic filopodia increase as development progresses. The dendritic filopodia soon explore most of the length of the corresponding hemisegment in the anteroposterior axis, sometimes overlapping with the dendrites of the neighboring Basins. Some of these branches do not retract, proceeding to stabilize into a secondary branch from which new filopodia can originate. Around 11 hours after the start of the imaging session, the filopodia exploration ceases and the neurons adopt their mature morphology. During this whole process the entire

VNC is gradually contracting, reducing the distance between segments and shrinking all neurons.

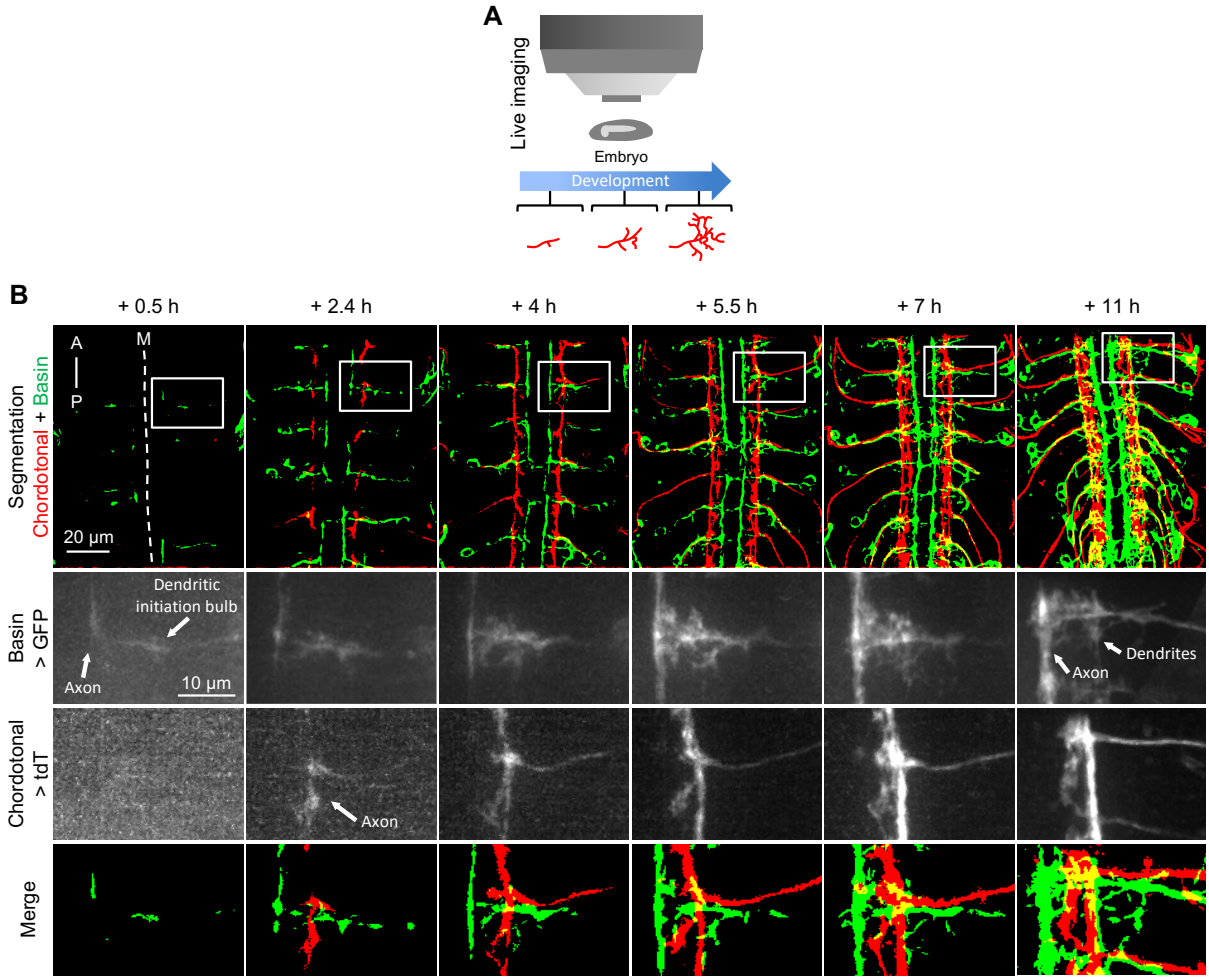

Figure 3.1. Chordotonal and Basin partner neurons establish contacts during embryonic development.

A) Schematic of the live imaging experiment. Chordotonal and Basin cells were imaged simultaneously in live embryos throughout development using a spinning-disk confocal microscope.

B) Developmental time lapse of Chordotonal (red) and Basin (green) cells. The images are confocal Z-projections of a ventral view of the VNC of live embryos. Time points are relative to the start of the imaging session due to the difference in temperatures before (25 °C) and during imaging (23 °C). The imaging session started 13 hours AEL (time point + 0 h), which is around the moment of earliest detectable expression of GFP in Basin cells. The earliest Basin morphology shows the main branch projecting medially

from the cell body to the anteroposterior tract where the axon will form. The swelling in between the Basin cell body and the axon is where the dendrites will branch from. The earliest expression of tdT in the Chordotonal axons was detected around 1 hour after the start of the imaging session. At this moment, the immature Chordotonal axons are already located in the anteroposterior tract where they will span. First row shows the whole imaging field of view, subsequent rows show the respective sub regions marked with a white square. Note that the central nervous system normally contracts during development, gradually shifting anteriorly. Due to stochasticity in the driver lines, not all neurons are labelled in all segments. The segmented versions of the light images are included for visual aid, in which Basins are shown in green and Chordotonals in red. Live embryos of the genotype *w; Basin-LexA, LexAop-GFP, mhc[1]; Ch-GAL4, UAS-tdT* (fly line 2, **Table 1)** were imaged. Dashed line represents the midline (M).

Embryonic development of Chordotonal axon terminals

I labeled the Chordotonal neurons with myristoylated tdTomato (tdT) under the regulation of the *iav-GAL4* driver. I observed the earliest moment of fluorophore detection in the Chordotonal axon terminals around 1 hour after the beginning of the imaging session (see **Figure 3.1B**), shortly after the earliest detection of Basin cells. At this moment, the Chordotonal axons were already located in their target anteroposterior tract, where they normally arborize. The lch5 Chordotonals in the intersegmental nerve are detected first, followed by the ones in the segmental nerve. The developing axons proceed to extend exploratory filopodia in their immediate vicinity, as they extend anteriorly and posteriorly. This is similar to the Basin axon exploration however, Chordotonal axons are located more laterally and ventrally from Basins. Unlike Basin axons, individual Chordotonals do not extend far in the anteroposterior axis. The ipsilateral axons eventually overlap and collectively form a continuous and sharp lateral edge, parallel to the midline. The medial side of the axons contains more branches and forms a more irregular edge.

Exploration of Basin dendrites and Chordotonal axons

As Chordotonal and Basin neurons develop, they extend short-lived exploratory filopodia until they eventually stabilize some of these branches and adopt their mature morphology. During this process, neurons explore their environment and come into contact with many other partner and non-partner cells.

Basin dendrites perform extensive exploration by extending multiple filopodia, covering a broad area within their hemisegment (see **Figure 3.A**). The exploration begins with small filopodia branching off the dendritic initiation point on the primary neurite. These filopodia extend and retract continuously, making this process very dynamic. The size of new filopodia increases and the exploration coverage area expands. Shortly after, multiple branches stabilize and the exploration slows down until the neurons adopt their mature morphology. Interestingly, the area covered during this dendritic exploration is larger than the area covered by the mature dendrites at the end of the exploration (see **Figure 3.A**), with the exploratory filopodia covering three times the area occupied by the mature dendrites (see **Figure 3.C**). This is also true for Chordotonal neurons (see **Figure 3.B**), with the exploratory axonal filopodia covering about 1.5 times the area of the mature axons (see **Figure 3.C**). However, the Chordotonal axon exploration is much more spatially reduced compared to Basins, and it is almost identical to the area collectively occupied by the mature axons (see **Figure 3.B**). This phenomenon (less extensive exploration) is observed in Basin axons as well (see **Figure 3.A**), suggesting it might be a property intrinsic to axons.

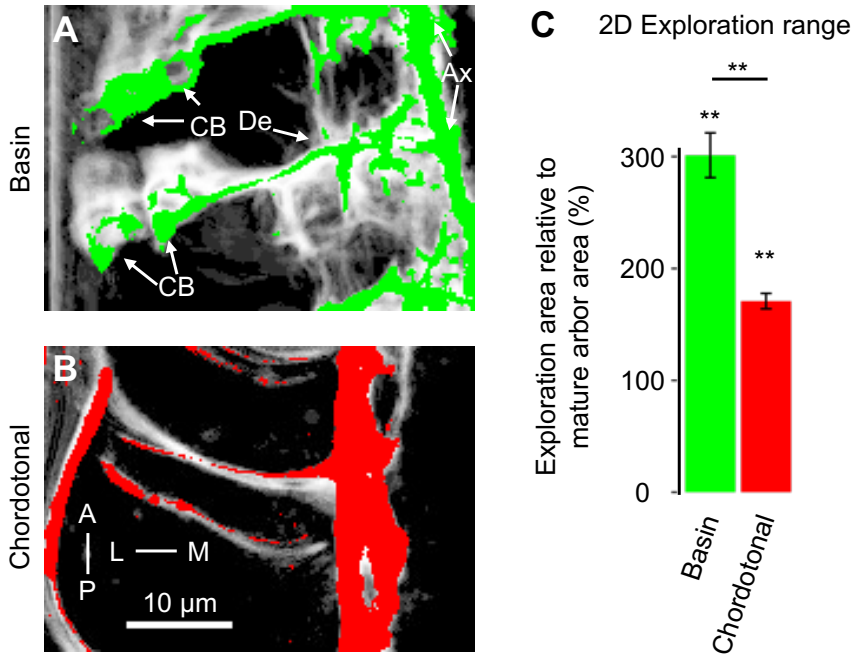

Figure 3.2. Basin dendrites explore more extensively than Chordotonal axons during embryonic development.

A-B) Time projections of the embryonic development of Basin (A) and Chordotonal (B) neurons. Animals of the genotype *w; Basin-LexA, LexAop-GFP, mhc[1]; Ch-GAL4, UAS-tdT* were imaged (fly line 2, **Table 1**).

A) Two Basin cells in one hemisegment during embryonic development. The dendrites of Basin cells explore (white) extensively along their hemisegment. They project exploratory filopodia to cover almost their entire hemisegment, sometimes reaching the exploration zone of the Basins in the next segment. The Basin axons explore much less compared to their dendrites. The mature Basins cease exploring to adopt a final morphology (green) that is much more compact than the exploration area. CB, cell body; De, dendrites; Ax, axon.

B) Chordotonal axons in one hemisegment during embryonic development. The Chordotonal exploration area (white) is limited almost exclusively to the area where the mature axons (red) will be present.

C) Two-dimensional exploration area covered during development relative to the area occupied by the mature arbors. Basin dendrites and Chordotonal axons covered a wider cumulative area during developmental exploration than the area occupied by their respective mature arbor (stars above each bar; one-sample t-test with default value of 100%). However, the relative exploration range of Basin dendrites is bigger than that of Chordotonal axons (Wilcoxon test). n= 10 hemisegments each.

Discussion

In this chapter I described experiments that allowed me to observe the development of synaptic partner neurons in the VNC of the live *Drosophila* embryo. This unveiled the dynamic exploratory process that axons and dendrites undergo to establish connections and form functional circuits. It revealed interesting differences in the range of exploration performed by axons and dendrites that help us better understand the formation of neural circuits.

There are several challenges associated with the live imaging of the development of neurons in the embryonic CNS. Neurons in the embryo are very small compared to those in later stages. Most of the driver lines that are known to label neurons of interest are characterized in the larval or adult stages. Therefore, it is necessary to first find lines that have the appropriate expression pattern in the embryo as well. Visualizing neurons at early embryonic stages is particularly difficult because of the initial low transgene expression levels. Additionally, to capture the entirety of the development of the neurons, it is necessary to track the embryos for multiple hours, which also makes the protocol and set-up technically challenging. Nevertheless, I successfully recorded the development of Basin and Chordotonal neurons in the live embryo.

Difference in dendritic and axonal explorations suggest dendrites seek out their partner axons

Basin neurons project dendritic filopodia that extensively explore their surroundings. Some of these filopodia are stabilized to adopt their mature morphology. The Basin dendritic exploration range is wider than the area the mature dendrites normally occupy. Thus, the filopodia that projected beyond the area occupied by the mature dendrites were not stabilized and were lost during development. The mature dendrites occupy more restricted areas, where the axon terminals of their presynaptic partners are known to be present from EM reconstructions (Jovanic et al., 2016; Ohyama et al., 2015).

Dendrites appear to explore a broad area, but only stabilize those filopodia that contacted their specific partners. Those filopodia that were not retained may not have received required signals for stabilization from their specific synaptic partners. This suggests that the dendritic exploration zone is independent of the location of the synaptic partners.

In contrast to dendritic exploration, the area occupied by axonal exploratory filopodia during development is almost the same as the area occupied by mature Chordotonal axons. This is the opposite of what I observed in the dendritic exploration of Basin cells but consistent with the exploration of the Basin axons (see **Figure 3.2**). These results suggest that dendrites might search for presynaptic axons, and not the other way around. This is consistent with previous findings that show branching and termination of sensory axons are regulated by the expression of receptors for positional guidance cues (like Slit, Semaphorins and Netrins) independently of their partners (Zlatic et al., 2003, 2009). The axon terminals, whose location is regulated by the global positional cues, appear to provide the instructive signal for postsynaptic dendrites to stabilize those filopodia that contact them.

Chapter 4

The role of positional cues and partner-derived cues in synaptogenesis

Introduction

In order to form connections, the presynaptic axon terminals and the postsynaptic dendrites of partner neurons must be in the same location where they can establish physical contact with each other. Therefore, in principle, simply guiding presynaptic axons and their postsynaptic dendrites to a common location through global positional cues could be sufficient to establish connections. Peters' rule is a hypothesis that intends to predict connectivity among neuron types based on the anatomical colocation of their axonal and dendritic arbors (Peters and Feldman, 1976; Rees et al., 2017). It suggests that the existence of connections between any two given neurons depends of the extent their dendrites and axons overlap. This has led to the idea that the connectivity between neurons is a consequence of their locational coincidence.

Indeed, gradients of global positional cues have been shown to regulate the targeting and termination of sensory axons in insects (Hong and Luo, 2014; Timofeev et al., 2012; Zlatic et al., 2003, 2009). In the vertebrate spinal cord, scrambling the location of motoneuron dendrites that are postsynaptic to sensory axons, does not affect the target location of sensory terminals (Sürmeli et al., 2011), indicating that these are also following specific positional cues. These studies suggest that sensory axons do not seek out their target dendrites, instead they seek out a specific 3D location.

However, detailed reconstructions of neuronal maps have shown evidence of striking synaptic specificity (Gerhard et al., 2017; Helmstaedter et al., 2013; Jovanic et al., 2016; Kasthuri et al., 2015; Lee et al., 2016; Ohyama et al., 2015; Schneider-Mizell et al., 2016; Takemura et al., 2013, 2015; White et al., 1986; Zheng et al., 2018) that suggests neurons are capable of discriminating the available cells and connecting only with a subset of them. These studies support Sperry's chemoaffinity hypothesis, which claims there are partner-derived

cues that guide the establishment of connections (Sperry, 1963). Thus, positional cues could guide only the presynaptic axons to branch and terminate in a specific location, while postsynaptic dendrites could seek out their presynaptic partners by searching for specific partner-derived cues. Indeed, live imaging experiments described in the previous chapter revealed that dendritic filopodia undergo much more extensive exploration than axons, suggesting axons may provide instructive signals for postsynaptic dendrites to stabilize their filopodia and connect to them. If this is true, we would expect that postsynaptic dendrites would be able to connect to their appropriate presynaptic partners, regardless of their location, as long as they are within the range of exploratory dendritic filopodia.

I therefore designed experiments to test the roles of positional guidance cues and putative partner-derived cues in the establishment of synaptic specificity. Specifically, I asked whether the postsynaptic dendrites would be able to find their presynaptic axons, even if the axons have been shifted to an ectopic location. I achieved this by increasing the sensitivity of the presynaptic sensory neurons to a positional cue that guides the placement of axons in the mediolateral axis of the VNC.

I generated a shift of location of the Chordotonal axons by overexpressing the chimeric receptor FraRobo (Bashaw and Goodman, 1999) in them. FraRobo consists of the ectodomain of the receptor Frazzled, and the intracellular domain of Robo (see **Figure 4.1A**). As mentioned before, Frazzled binds to the midline-attractant Netrin and mediates axonal attraction to the midline (Kolodziej et al., 1996). Robo binds to Slit and mediates repulsion to the midline (Brose et al., 1999; Kidd et al., 1998a, 1999). Therefore, FraRobo has chimeric properties derived from its parent receptors by binding to Netrin and mediating repulsion to it (Bashaw and Goodman, 1999).

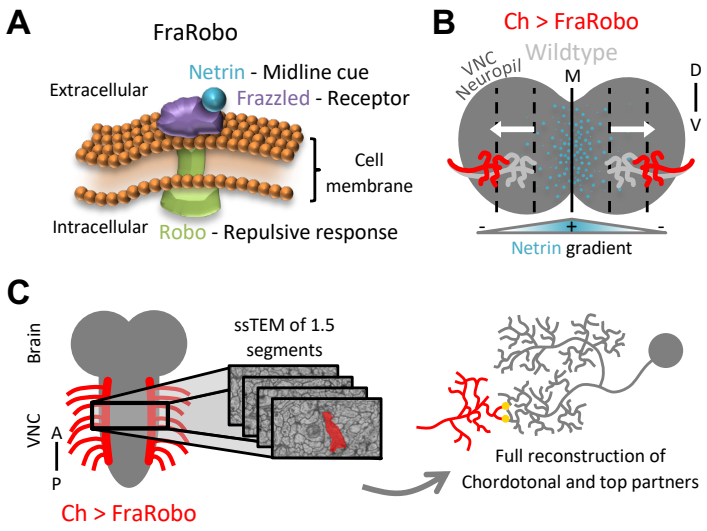

Figure 4.1. Chordotonal neurons expressing FraRobo are repelled from the midline.

A) FraRobo is a chimeric receptor with the ectodomain of Frazzled (purple) and the intracellular domain of Robo (green). The Frazzled component binds to Netrin (blue) while the Robo fraction triggers a repulsive response.

B) Netrin (blue) is secreted at the midline of the neuropil (dark gray), creating a concentration gradient in the mediolateral axis with the highest concentration at the midline (M) and the lowest at the lateral ends. The Chordotonal (Ch) axons that ectopically express FraRobo (red) are more sensitive to Netrin and avoid areas of high concentration of it, resulting in a lateral shift compared to wildtype Chordotonal axons (light gray).

C) 1.5 segments of the VNC of an animal expressing FraRobo exclusively in the Chordotonal neurons was imaged using serial section transmission electron microscopy (ssTEM). Chordotonal neurons and their top partners were fully reconstructed to investigate the possible effects of this manipulation on morphology and connectivity.

The ectopic expression of FraRobo in the Chordotonal neurons is therefore expected to produce a lateral displacement of their axon terminals mediated by their repulsion from the midline attractant Netrin (see **Figure 4.1B**). This would enable me to test the role of partner location in wiring specificity and quantify the effects of this positional manipulation on the connectivity of Chordotonal neurons with their postsynaptic partners.

Results

EM reconstruction of shifted Chordotonal neurons and their postsynaptic partners

The best way to confidently determine if there are any connectivity effects of the displacement of the Chordotonal axons is to look at any morphological changes and measure the number of connections with their synaptic partners. EM reconstruction of neurons would provide morphological and connectivity information about the circuit effects of this manipulation. Therefore, I performed EM reconstruction of the Chordotonal neurons and their key postsynaptic partners in a first instar larva, in a volume spanning one and a half segments of an animal in which Chordotonal axons selectively expressed FraRobo (*w;; iav-GAL4/UAS-FraRobo*) (see **Figure 4.1C**).

The Chordotonal axons expressing FraRobo were shifted laterally, as expected, closer to the edge of the neuropil and away from the midline (see **Figure 4.2C** and **Figure 4.2E**). The axons grouped together in semi-isolated lateral clusters, losing the continuous arrangement in the anteroposterior axis that is normally observed between segments (see **Figure 4.2B** and **Figure 4.2D**). The expression of FraRobo affected the Chordotonal axons with different magnitudes, causing Chordotonals from some segments to shift more than others. This resulted in some axons not shifting or occupying both their normal location and the shifted one. I measured the overall mediolateral shift of the Chordotonal axons observed in this EM volume by quantifying the node density of the resampled reconstructed neurons in this axis and comparing it to a control. The distance in the mediolateral axis was normalized by the total length of the neuropil to account for differences in size between EM volumes. The relative distance between the mediolateral positions of highest node density in the right and left sides was 19.2% higher than in the control animal (see **Figure 4.2F**). The difference in the distance between contralateral axons in the right and in the left sides of normal and shifted Chordotonals corresponds to 10% of the total length (maximum distance in the mediolateral axis) of the neuropil.

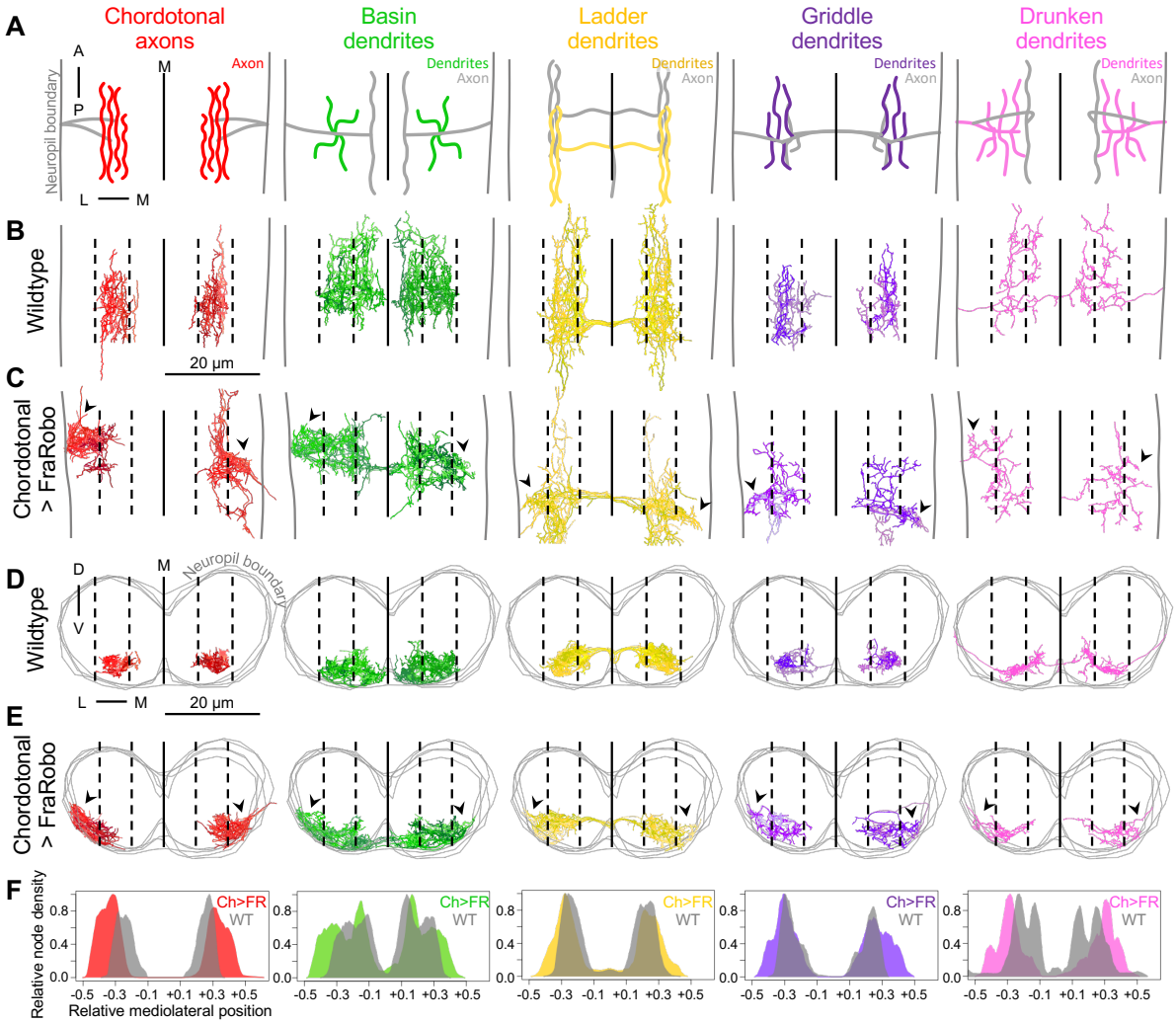

Figure 4.2. Postsynaptic dendrites extend ectopic branches to reach for the displaced Chordotonal axons.

A) Schematic of a dorsal view of the Chordotonal axons and the dendritic regions of their postsynaptic partners in one abdominal segment. The colored subcellular regions are consistent with those displayed in subsequent images in this figure.

B-E) Dorsal (B and C) and cross section (D and E) views of the reconstructed Chordotonal axons and postsynaptic partner dendrites in wildtype (B and D) (*w1118*) and in a sample in which Chordotonals express FraRobo (C and E) (*Ch-GAL4 > UAS-FraRobo*). Chordotonal axons expressing FraRobo are displaced laterally (arrowheads), away from the midline (M; solid line), reaching the edge of the neuropil. The postsynaptic partners display ectopic branches in lateral domains (arrowheads) as a consequence of the displacement of their presynaptic partner. The neuropil boundary is represented by either a pair of gray vertical lines for dorsal views (B and C) or gray consecutive rings for cross section views (D and E). Dashed lines split the maximum width of the neuropil in six equidistant sections, three on either side of the midline.

F) Node density distribution of reconstructed neurons in the mediolateral axis. The node density of all the reconstructed neurons was quantified using a 2.5 μm sliding window across the mediolateral axis. The mediolateral positions are normalized to the width of the neuropil of the corresponding EM volume. The midline is represented by zero in the x-axis. The node densities are normalized to the maximum density of the respective cell type.

Postsynaptic dendrites follow shifted presynaptic axons

The displacement of the Chordotonal axons had a morphological effect in their postsynaptic partners, Basin, Ladder, Griddle and Drunken neurons. The excitatory Basin neurons normally receive Chordotonal input in the medial and lateral subregions of their dendritic arbor. Surprisingly, when the Chordotonal axons were shifted laterally, Basins broadened their dendritic coverage by spreading out their dendrites laterally to reach for the ectopic Chordotonal input (see **Figure 4.2C** and **Figure 4.2E**). Basin dendrites can now be found all the way to the edge of the neuropil, occupying a location where they are normally absent. Ladders are inhibitory interneurons and predominately downstream of Chordotonal neurons. When the Chordotonal axons were shifted laterally, Ladders extended additional dendrites to reach for the Chordotonal input (see **Figure 4.2C** and **Figure 4.2E**). The Ladder dendrites were overall reduced in size, suggesting these neurons are greatly impacted by the displacement of their main upstream partners. A morphological adaptation was also observed in the dendrites of Drunken and Griddle neurons, inhibitory downstream partners of Chordotonals, but to a lesser extent. Both, Drunken and Griddle, extended extra dendritic branches to reach for ectopic Chordotonal input (see **Figure 4.2C** and **Figure 4.2E**), similarly to Ladder neurons.

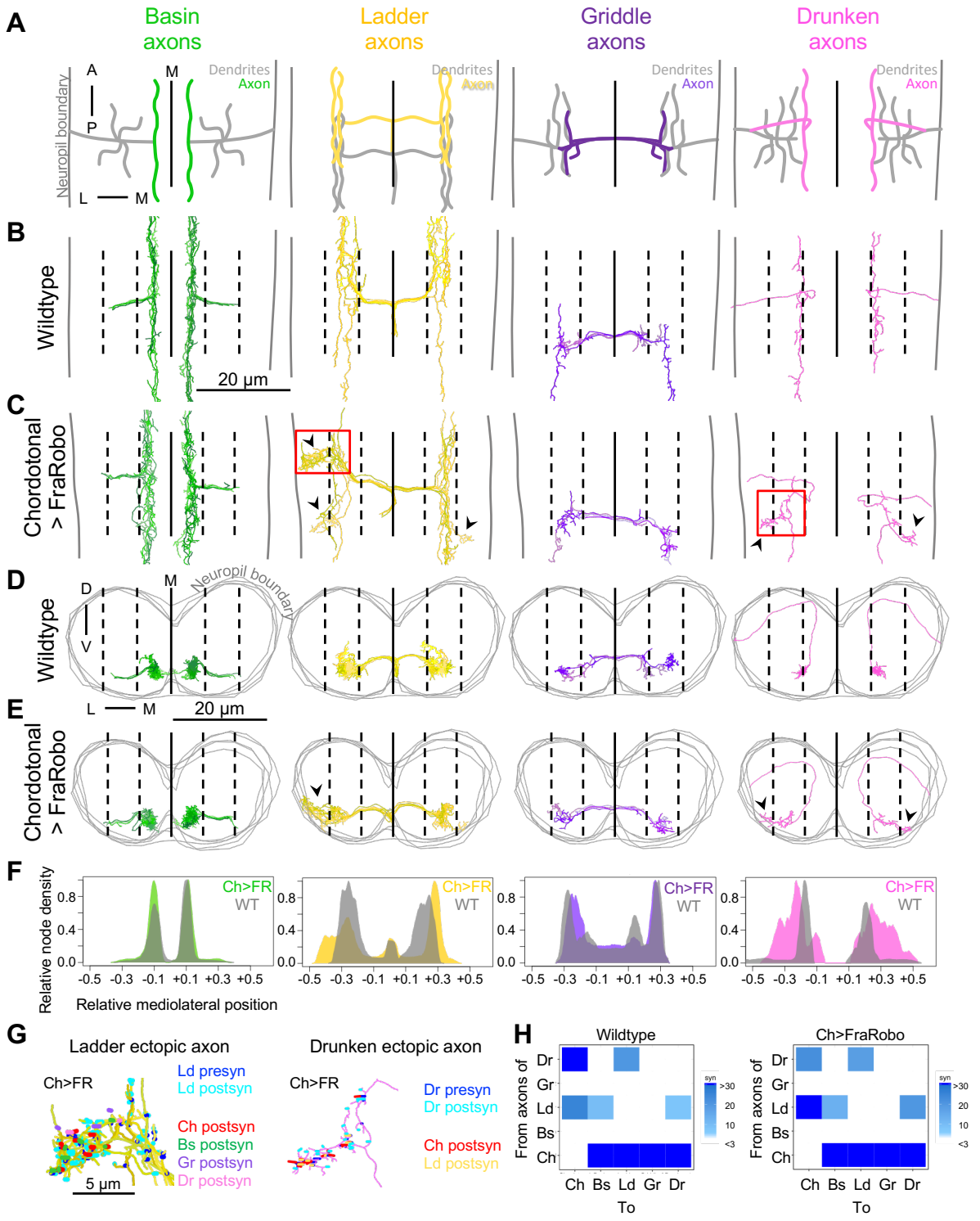

Figure 4.3. Interneuron axons reach for displaced Chordotonal axons, independently of their dendrites.

A) Schematic of a dorsal view of the dendritic regions of the Chordotonal postsynaptic partners in one abdominal segment. The colored subcellular regions are consistent with those displayed in subsequent images in this figure.

B-E) Dorsal (B and C) and cross section (D and E) views of the reconstructed axons of Chordotonal partners in wildtype (B and D) (*w1118*) and in a sample in which Chordotonals express FraRobo (C and E) (*Ch-GAL4 > UAS-FraRobo*). The axons of Ladder and Drunken extend ectopic branches (arrowheads) due to the displacement of the Chordotonal axons. However, Basin and Griddle axons do not display any lateral displacement. The neuropil boundary is represented by either a pair of gray vertical lines for dorsal views (B and C) or gray consecutive rings for cross section views (D and E). Dashed lines split the maximum width of the neuropil in six equidistant sections, three on either side of the midline (M; solid line).

F) Node density distribution of reconstructed axons in the mediolateral axis. The node density of all the reconstructed neurons was quantified using a 2.5 μm sliding window across the mediolateral axis. The mediolateral positions are normalized to the width of the neuropil of the corresponding EM volume. The midline is represented by zero in the x-axis. The node densities are normalized to the maximum density of the respective cell type.

G) The ectopic axonal branches of Ladder and Drunken (red squares in C) are presynaptic to Chordotonal axons and to other Chordotonal partners. This means that the axonal shift of Ladder and Drunken could be directly caused by the shifted Chordotonal axons or by the indirectly-shifted interneurons.

H) Connectivity matrix of axon-to-whole-neuron connections between Chordotonal (Ch), Basin (Bs), Ladder (Ld), Griddle (Gr) and Drunken (Dr). Axons of Basin and Griddle do not normally synapse onto each other or any neuron that was displaced as a consequence of the expression of FraRobo in Chordotonals (i.e. Chordotonal, Ladder or Drunken). Only including connections between cell types with at 3 or more synapses to a single neuron.

Since most of the Chordotonal synapses onto their key postsynaptic partners are located in the interneuron dendritic compartments (axo-dendritic connections), it is unclear whether the location of the interneuron axons would also be shifted, as were the dendrites. Additionally, previous work shows that sensory axons can be displaced regardless of their postsynaptic partner. This raises the possibility that interneuron axons and dendrites might use different guidelines when they are placed in a specific location during development. To investigate this further, I looked at the morphology and location of the axons of the Chordotonal partners (see **Figure 4.3**). The lateral shift of the Chordotonal axons caused a subsequent shift in some of the axons of key downstream partners. The axons of Ladder and

Drunken showed clear ectopic branches that overlap with the shifted Chordotonal axons, while the axons of Basin and Griddle did not show any displacement (see **Figure 4.3C** and **Figure 4.3E**). Interestingly, the ectopic axonal branches from Ladder and Drunken are also presynaptic to Chordotonals and some of the other shifted interneuron dendrites (see **Figure 4.3G**). This suggests these ectopic axons would have been shifted to reach for the ectopic Chordotonals, interneurons or both. The axons of Basins and Griddles, which were not displaced, do not normally form synapses with Chordotonals or any of the other interneurons that were shifted (see **Figure 4.3H**). This explains why the location of these axons was not affected. The difference in the shift of dendritic and axonal compartments within the same cell shows that dendrites and axons use independent placement guidelines.

As mentioned before, the effect of expressing FraRobo is variable and can affect some neurons more than others. While this variability was expected, it served as an internal (same sample) control of the downstream effects of this manipulation. In the EM volume where the Chordotonal neurons expressed FraRobo, the Chordotonal axons in one hemisegment (upper right in **Figure 4.2C**) show a partial lateral shift. As a result, Ladder neurons did not show any extra lateral branches in this specific hemisegment (see **Figure 4.3C** and **Figure 4.3E**). However, these same neurons had ectopic branches reaching for Chordotonal input in all the other hemisegments that were imaged. This serves as a control to show that the formation of ectopic dendrites in Ladder neurons is directly due to the lateral displacement of their main presynaptic partner, the Chordotonal neurons. This effect is particularly easy to visualize in Ladder dendrites since their ectopic branches project away and perpendicularly from the rest of their dendritic arbor. However, the variability of the Chordotonal shift in Basin dendritic coverage is not as visually obvious.

Shifting sensory axons alters structural connectivity within the circuit

EM reconstruction of Chordotonal neurons and their postsynaptic partners enabled me to quantify the effects of experimental manipulations on synapse numbers, and not just on morphology of dendritic arbors. Mapping the synapses from all Chordotonals shows that the displaced axons do connect to their postsynaptic partners (see **Figure 4.4A-C**). However, the ranking of the Chordotonal partners was significantly redistributed. In wildtype, Ladder and

Griddle are the predominant top partners (by total input) of Chordotonals. Conversely, Basins are the top partner of FraRobo-expressing Chordotonals, while Ladders are further down the ranking. On top of changing the order in the ranking of Chordotonal partners, it is possible that the lateral displacement of Chordotonal axons led to the loss of some postsynaptic partners. There is a decrease in the total number of postsynaptic partners in the FraRobo EM volume. However, it is believed to be at least partially because it is a slightly younger animal, having smaller neurons with fewer synapses. Therefore, Chordotonal neurons in this volume have fewer partners, including fewer noisy connections to weakly connected neurons. Interestingly, most of strongly connected Chordotonal partners in wildtype remain connected in the FraRobo volume (see **Figure 4.4B** and **Figure 4.4C**). Alternatively, the lateral shift of Chordotonal axons could also lead to the gain of new synaptic partners at their new location. In fact, only a single neuron was found to be connected in the FraRobo volume that was not a regular Chordotonal partner in the wildtype (see **Figure 4.4C**). This new partner was weakly connected and barely above the connectivity threshold (at least 3 synapses on each side). The low number of new partners and the retention of strongly connected partners shows remarkable partner specificity.

Since the total number of synapses in the nervous system increases throughout development of the larva, it is not possible to use this measurement to accurately compare connectivity strength across different EM volumes. However, the fraction of input a neuron receives from (or makes onto) a specific partner has been shown to be remarkably conserved across individuals and development (from first to third instar larva in *Drosophila*) (Gerhard et al., 2017). Therefore, throughout this study I will report connectivity between partner neurons (for example: neuron A synapsing onto neuron B) as a fraction, resulting from dividing the number of shared synapses by the total postsynaptic input (synapses from A to B/total incoming synapses of B). Using fractions of synapses, rather than absolute numbers, allowed me to account for slight differences in age between the samples used to generate the EM volumes.

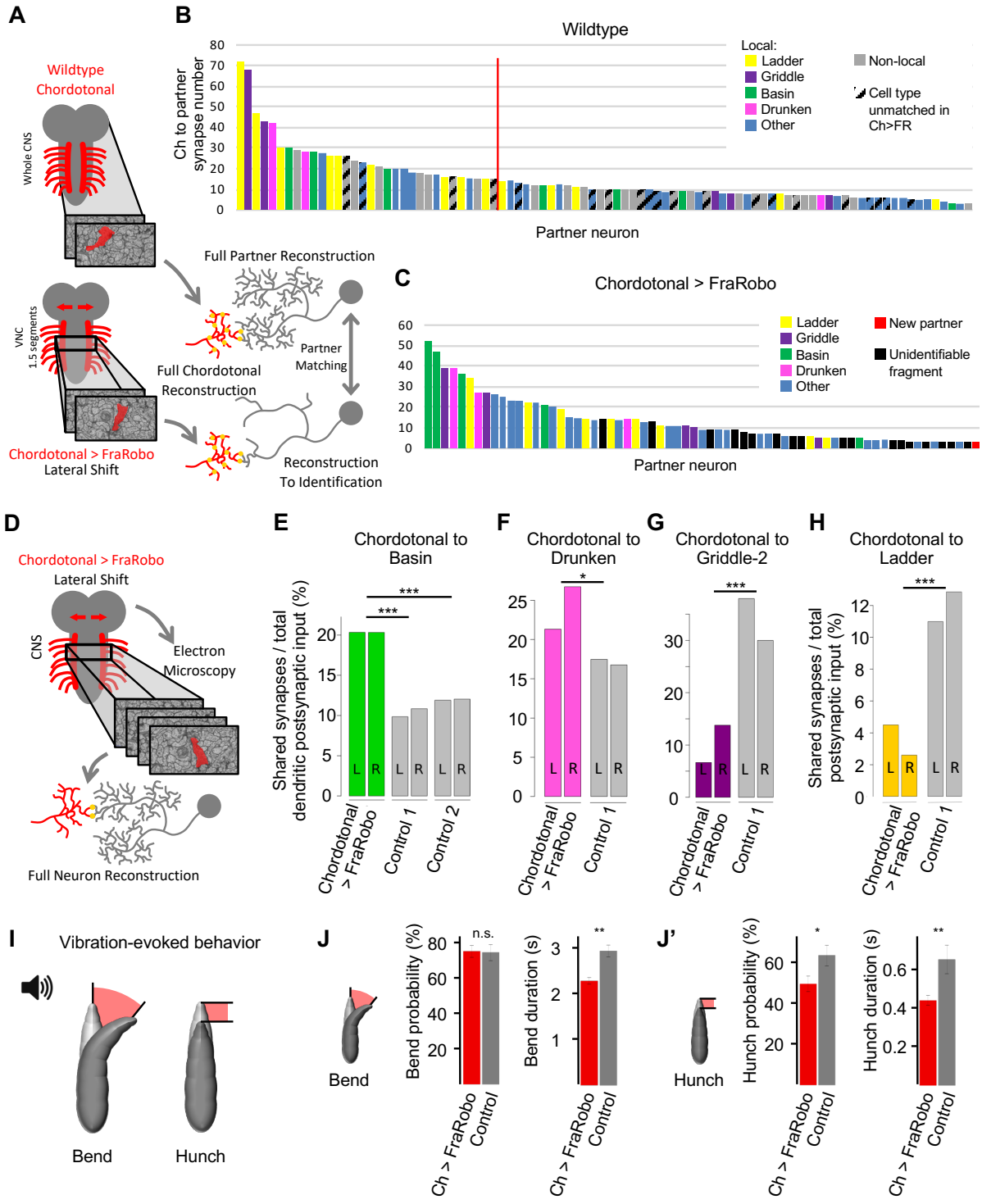

Figure 4.4. Shifting the location of the Chordotonal axons alters the circuit connectivity, generating deficient mechanosensory behavior.

A) Chordotonal neurons and downstream partners were reconstructed in two different EM volumes: one wildtype (*w1118*) and one in which the Chordotonals expressed FraRobo (*Ch-GAL4 > UAS-FraRobo*). The

wildtype volume encompasses the whole CNS, and most of the partners downstream of Chordotonals in it have been fully reconstructed. The FraRobo volume consists of approximately 1.5 abdominal segments. In this volume, the non-key (i.e. not Basin, Ladder, Griddle, and Drunken) Chordotonal partner neurons were partially reconstructed up to a point where they could be identified and matched to fully reconstructed neurons from the wildtype volume.

B-C) Connectivity plots of the downstream partners of Chordotonal neurons from one hemisegment in a wildtype EM volume (B) and a *Ch-GAL4 > UAS-FraRobo* volume (C). Bars represent individual neurons. Number of synapses shown are from all eight grouped Chordotonal axons onto individual postsynaptic partners.

B) Local neurons were defined as those within the same region (same segment and half of the two adjacent segments) as Chordotonals (limits set to approximate those of the FraRobo volume). Those neurons partially within these limits were considered as local if the encompassed fractions could still be identified, otherwise they were considered as non-local. Those cell types that were not found downstream of Chordotonal neurons in the FraRobo volume are marked as unmatched. Only those neurons with at least 3 synapses from Chordotonals on each side (left and right) of the segment are shown. Red vertical line indicates the threshold between neurons strongly ($\geq$15 total synapses) and weakly ($<$15 total synapses) connected to Chordotonals.

C) The ranking of Chordotonal downstream partners is redistributed compared to wildtype. Most of top local partners (from B) remain connected when Chordotonals were shifted. Partial fragments of neurons that leave the EM volume that could not be identified are colored in black (correspond to “unmatched” in B). Neurons downstream of Chordotonals in the FraRobo volume (reproducible in left and right) that are not downstream Chordotonals in the wildtype volume are marked in red. Only those neurons with at least 3 synapses from Chordotonals are shown.

D) Chordotonals and their key downstream partners (Basin, Ladder, Griddle and Drunken) were fully reconstructed in a *Ch-GAL4 > UAS-FraRobo* EM volume of 1.5 segments.

E-H) Connectivity between FraRobo-expressing Chordotonal neurons and key postsynaptic partners is altered. The number of synapses from Chordotonals onto the dendrites of the postsynaptic partner was divided by the total number of dendritic inputs of the postsynaptic partner (E-G), or total postsynaptic input (H; dendritic and axonal input considered for Ladder due to strong Chordotonal input onto both subcellular compartments). Connectivity from neurons in the right (R) and left (L) sides of one segment is shown separately. However, synapse counts from right and left were grouped for statistical analysis.

I) Sound-generated vibration activates Chordotonal neurons and elicits bending and hunching behaviors.

J-J') Animals with shifted Chordotonal axons have deficient mechanosensory behavioral responses. The probability of turning behavior in animals with shifted Chordotonals is similar to that of controls but with longer duration (J). However, the probability and duration of hunch are both increased in animals with shifted Chordotonals (J'). Error bars represent the 95% confidence interval for probabilities or standard error for durations. For probabilities: experimental (red) n= 677; control (gray) n= 367. For duration: experimental (red) n= 506; control (gray) n= 272.

I found that the fraction of Basin synapses from Chordotonal neurons was higher than in control volumes (see **Figure 4.4E**). A similar increase in connectivity was also observed for Drunken neurons (see **Figure 4.4F**). Contrastingly, the fraction of Griddle input from Chordotonal neurons was lower than control (see **Figure 4.4G**). Basin, Drunken and Griddle receive most of their Chordotonal input onto their dendrites, which are fully contained in the FraRobo volume. However, Ladders normally receive a significant amount of Chordotonal input onto both, their dendrites and axons. Therefore, the fraction of total (axonal and dendritic) Ladder input synapses was calculated. Since parts of the Ladder arbors exited the FraRobo EM volume, equivalent (in coverage) subvolume limits were used to restrict the total number of Ladder input synapses considered in the wildtype volume. This correction made it possible to compare Ladder connectivity fractions between wildtype and FraRobo volumes. This revealed that the fraction of Ladder input from Chordotonal decreased when Chordotonal neurons had been shifted laterally by the expression of FraRobo (see **Figure 4.4H**). Altogether, I found that Basins and Drunkens receive a higher relative number of synapses from Chordotonal neurons compared to controls. Conversely, while Ladders and Griddles do establish connections with the shifted Chordotonal axons, the fraction of synapses from Chordotonals onto them was lower than in controls. The distribution of Chordotonal synapses onto Ladder and Griddle was also affected (See **Figure S3**). The same connectivity effects are found when the synapse counts are normalized by postsynaptic arbor length (see **Figure S1**).

Thus, the EM reconstruction of the partners of Chordotonal neurons revealed that dendrites and axons of interneurons are able to find and connect to the Chordotonal axons, even when these have been shifted to ectopic locations. However, the analysis of detailed synaptic connectivity in such animals revealed that the relative fractions of input onto different postsynaptic neurons are significantly different to wildtype.

The circuit with shifted mechanosensory axons is functional, but not normal

I performed behavioral experiments to test whether the differences in synaptic connectivity observed in the EM volumes would have an effect on the animal's responses to mechanosensory stimuli (see **Figure 4.4I**). I found that third instar larvae with FraRobo-expressing Chordotonal axons display body-bending behavioral responses to vibration, but the responses were significantly shorter compared to controls (see **Figure 4.4J**). Similarly, these animals responded to vibration by hunching, but the probability and duration of this behavior were both significantly lower than in controls (see **Figure 4.4J'**). This shows that despite the displacement of the Chordotonal neurons, the mechanosensory circuit is still functional and capable of generating mechanically-evoked behavior. However, the overall circuit connectivity was altered by the locational shift of Chordotonal axons, generating deficient behavioral responses (see **Figure 4.5**).

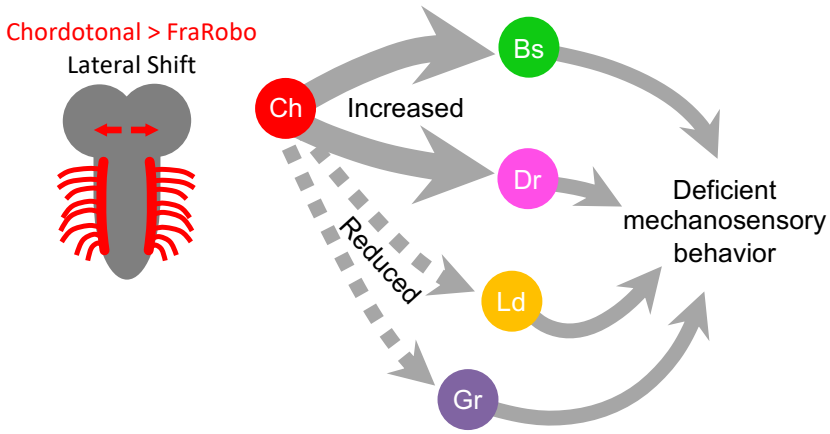

Figure 4.5. The lateral displacement of Chordotonals leads to an overall connectivity imbalance that generates deficient mechanosensory behavior.

The expression of FraRobo in Chordotonal neurons causes a lateral shift of their axons. This displacement leads to an increased connectivity with Basin and Drunken neurons, while the connectivity with Ladder and Griddle are reduced. Overall, this change in connectivity generates a deficient behavioral response to mechanical stimuli.

Discussion

In this chapter I investigated the role of location of partner neurons and of partner-derived cues in the specificity of the synaptic connections between them. I induced the ectopic expression of FraRobo in the Chordotonal neurons and generated a lateral displacement of their axons in the nerve cord. This experiment allowed me to test Peters' rule and see whether locational coincidence in fact dictates connectivity. If Peters' rule were true, Chordotonal axons would now connect to a new set of partner neurons available in their new location. Connectivity with their regular synaptic partners would be lost or significantly reduced. The morphology of the regular downstream partners would be expected to remain unchanged, as they also connect to new presynaptic neurons.

Surprisingly, most of the strongly connected Chordotonal partners remain connected even when the Chordotonal axons were displaced. However, the ranking of partners is different, resulting in a redistribution of Chordotonal output. Strikingly, I found only one new partner and it receives very little input from the shifted Chordotonals. This suggests there is partner specificity that prevents the shifted Chordotonal axons from strongly connecting to any newly available neurons.

Surprisingly, the downstream partners Basin, Ladder, Drunken, and Griddle responded to this manipulation by modifying their dendritic morphology to receive ectopic Chordotonal input. Basin cells broadened their dendritic arbors to increase their coverage, while Ladders

extended extra branches away from the rest of their dendrites. This is striking evidence that postsynaptic dendrites are capable of adapting their morphology in order to establish connections with their specific presynaptic partners. This proves there must be partner-derived cues these neurons are using during development to establish connections.

The readjustment of morphology of synaptic partners is consistent with a previous study done in the adult olfactory system of *Drosophila* (Zhu et al., 2006). This work showed that overexpressing Dscam in second-order projection neurons shifted the relative position of their dendrites to a different glomerulus in the antennal lobe. This change of location caused a corresponding shift of its presynaptic partner (olfactory sensory neurons) axons, maintaining the connection specificity. This is evidence that axons are capable of following postsynaptic dendrites. However, the directionality (axons follow dendrites) of this particular example might also be a result of the timing of developmental events, where the postsynaptic dendrites of the projection neurons innervate the developing adult antennal lobe before the arrival of the presynaptic axons (Jefferis et al., 2004). Conversely, another study showed that the dendrites of motoneurons in the *Drosophila* larva VNC can be displaced with the ectopic expression of Frazzled (Couton et al., 2015). This change in the location of dendrites led to a reorganization of the ratio of synaptic input these cells receive from upstream interneurons. However, the location of the presynaptic axons remained unchanged, showing that in this case the presynaptic axons do not follow postsynaptic dendrites. Together, these studies suggest that synaptic selectivity may be regulated differently across the CNS.

I found that even though postsynaptic dendrites found their shifted presynaptic axons and connected to them, they did not establish wildtype numbers of connections with their partners. Interestingly, some postsynaptic neurons received more synapses than in controls, and others fewer. The relative numbers of synapses from shifted Chordotonals onto Basins and Drunkens were greater than in controls, while the connections from Chordotonals onto Ladders and Griddles were reduced. This suggests some partners are more flexible and capable of adapting to this manipulation than others. The shift of the presynaptic partner therefore resulted in a change in the overall connectivity within the circuit, indicating that orderly positioning of presynaptic partners is important for normal circuit assembly, even if partner-derived cues do exist.

Consistent with the finding that postsynaptic dendrites are able to find and connect to shifted presynaptic axons, I found that animals expressing FraRobo in Chordotonal neurons do respond to vibration by bending their bodies and hunching, indicating the mechanosensory circuit is functional. However, consistent with the finding that the relative numbers of connections from shifted Chordotonals to different neurons were different than wildtype, I found that the behavioral response to vibration of such animals was lower than in controls. Specifically, two types of inhibitory neurons (Griddle and Ladder) received less synapses, while one excitatory (Basin) and one inhibitory (Drunken) received more synapses. However, since disinhibition has been shown to control many of the responses to mechanosensory stimuli in this circuit (Jovanic et al., 2016), the lower behavioral response could be explained by the reduction in the relative number of disinhibitory connections.

In summary, I found that interneuron dendrites and axons are able to find and connect to their partners even when these are in ectopic locations. This suggests that neurons use partner-derived cues that allow them to identify and connect to each other. However, without the orderly positioning of Chordotonal axon terminals set by global positional cues, the number of connections is altered with significant consequences on behavior. Therefore, global positional cues and partner-derived cues both contribute to proper circuit assembly in the developing *Drosophila* nerve cord.

Chapter 5

The role of developmental neuronal activity in synaptic specificity and circuit function

In this chapter I explore whether synaptic activity contributes to the establishment of appropriate synaptic connections. In chapter 3, I have shown that postsynaptic dendrites project long exploratory filopodia and establish their first contacts with sensory axon terminals during late embryonic development. These interactions begin right before the first action potentials happen in the developing nervous system of the *Drosophila* embryo (Baines and Bate, 1998). This raises the possibility that neuronal activity between developing neurons might contribute to wiring specificity, in addition to specific partner-derived molecular cues.

Motoneurons in *Drosophila* have been shown to use synaptic input to regulate the balance of their dendritic arbor size (Tripodi et al., 2008). Additionally, exploratory axonal filopodia contacting potential targets exhibit low frequency calcium oscillations that seem to be involved in the withdrawal of off-target contacts (Vonhoff and Keshishian, 2017a, 2017b).

In contrast, other studies suggest activity is not even required for the normal formation of circuits (Hiesinger et al., 2006; Jefferis et al., 2004; Scott et al., 2003; Sugie et al., 2018). A recent study showed that neither evoked nor spontaneous synaptic activity are required for the stabilization of motoneuron filopodia during metamorphosis in *Drosophila* (Constance et al., 2018). In fact, they show that muscle fibers do not even display robust calcium responses to the thermogenetic activation of motoneurons until after most of the motoneuron axon growth had occurred. This shows that the patterning of this circuit and the specificity of its connections are independent of synaptic communication between partners. These studies suggest synaptic activity during development might have different roles among different organisms, or even between circuits of the same organism.

To assess the role of developmental synaptic activity in partner specificity, I silenced the Chordotonal neurons during development and examined the effects of this manipulation on connectivity and function of the circuit in the larva. I used EM reconstruction, functional imaging, and behavioral assays to analyze the effect of this manipulation on the connections with specific partners and the overall behavioral output of the circuit.

Results

Lack of sensory input alters structural connectivity within the circuit

To investigate the role of synaptic activity during development in the establishment of synaptic specificity, I silenced the Chordotonal neurons through the targeted expression of tetanus toxin light chain (TNT) in them (Sweeney et al., 1995). TNT cleaves synaptobrevin and prevents evoked synaptic vesicle release, abolishing synaptic transmission. This manipulation permanently silenced the Chordotonal neurons, preventing evoked synaptic communication with any of their partners.

In order to assess the effect this manipulation has on the circuit's connectivity, I performed EM reconstruction of Chordotonals and their key downstream partners in an EM volume that spans 1.5 segments of a first instar larva with constitutively silenced Chordotonals (through selective TNT expression) (see **Figure 5.1A**). I found that silencing the Chordotonal neurons had an effect on the connectivity from Chordotonals onto Basin, Griddle, and Ladder neurons, albeit in opposite ways. EM reconstruction of these connections revealed that the fraction of Basin input synapses from inactive Chordotonals was higher than in controls (see **Figure 5.1B**). In contrast, the fraction of Griddle and Ladder input from Chordotonals was decreased (see **Figure 5.1C** and **Figure 5.1D)**, while there was no difference in the connectivity between Chordotonal and Drunken neurons (see **Figure 5.1E**). This shows the relative number of connections between silent Chordotonals and downstream partners was different across cell types.

Lack of sensory input alters functional connectivity with the circuit

Next, I wanted to test whether the significant differences in structural connectivity induced by silencing of sensory axons also result in differences in functional connectivity.

Since the Chordotonal neurons in this EM volume are permanently silenced with TNT, it is impossible to test whether the Chordotonal-to-Basin increase in connectivity is functional. I therefore genetically targeted the overexpression of temperature-sensitive Shibire (Shi^{ts1}) in the Chordotonal neurons. Shi^{ts1} is a dominant negative mutant version of the *Drosophila* ortholog of Dynamin (Chen et al., 1991). It reversibly blocks synaptic vesicle endocytosis at a restrictive temperature (≥30 °C), greatly reducing synaptic transmission (Kitamoto, 2001). The targeted expression of Shi^{ts1} allowed me to reversibly inactivate the Chordotonal neurons with temporal control.

I used Shi^{ts1} to reversibly silence Chordotonal neurons and generate an analogous manipulation to the inactivation with TNT. I restricted the silencing period by controlling the temperature at which the animals grew (see **Figure 5.1F**). I incubated the embryos at 31 °C (restrictive temperature) for the first 24 hours, then at 18 °C (permissive temperature) for another day until testing. In this way, I silenced the Chordotonal neurons during embryonic development and reactivated them in the early larval stage, giving the circuit ample time to be fully active before testing. I used this protocol to silence the Chordotonal neurons exclusively during development and test the functional connectivity between Chordotonal and Basin neurons in the larva. In order to observe Basin responses to Chordotonal activation, I expressed GCaMP6s (Chen et al., 2013), a fluorescent calcium indicator, in Basins to monitor their activity. At the same time, I used CsChrimson, a red-shifted channelrhodopsin (Klapoetke et al., 2014), to activate Chordotonal neurons with red light.

I found that Basin cells had greater calcium responses to the optogenetic activation of Chordotonals when they were inactive during development, compared to animals in which the Chordotonals had always been active (see **Figure 5.1G** and **Figure 5.1G'**). This is consistent with the observed increase in synapse numbers between TNT-inactivated Chordotonals and Basin neurons from the EM reconstructions (see **Figure 5.1B**).

I wanted to test whether this increased functional response persists along the circuit and could be detected downstream of Basin neurons. I therefore recorded calcium responses in A00c neurons, which are ascending neurons that collect Basin input along the nerve cord and project onto the brain. I also used CsChrimson to activate Chordotonals, GCaMP6s to record A00c calcium responses, and Shi^{ts1} to inactivate Chordotonals with the same silencing protocol as the experiment described above.

I found that the calcium responses of A00c axons in the brain to the optogenetic activation of Chordotonals had an increasing trend (but not statistically significant) when the Chordotonal neurons were inactivated with Shi^{ts1} (see **Figure 5.1H** and **Figure 5.1H'**). This shows that the increase in the number of structural connections induced by the developmental silencing of Chordotonal neurons is accompanied by an increase in the strength of the direct functional connections between Chordotonals and Basins, and possibly in the indirect (via Basins) functional connection between Chordotonals and A00c neurons.

Lack of sensory input alters the behavioral output of the circuit

Next, I wanted to test whether the significant differences in structural and functional connectivity induced by silencing of sensory axons also result in differences in the behavioral output of the circuit.

I measured the behavioral responses to vibration of first instar larvae in which the Chordotonal neurons were reversibly silenced during development (see **Figure 5.1I**), just as in the functional imaging experiments above. As stated before, Chordotonals are activated by vibration, and larvae stereotypically respond to this stimulus by bending their bodies and hunching (Jovanic et al., 2016; Ohyama et al., 2013, 2015). Therefore, I quantified the population probability of performing bending or hunching behaviors when stimulated with vibration.

I found that these animals had a reduced probability to respond to vibration (see **Figure 5.1J-** and **Figure 5.1J'**), compared to animals with Chordotonals that had always been active. This behavioral effect is still present in third instar larvae that grew for a longer period at the

permissive temperature after the same Chordotonal silencing period (see **Figure 5.1K** and **Figure 5.1K'**). This reduced behavioral response could potentially be explained by a reduction in the fraction of input from TNT-silenced Chordotonal neurons onto Griddles and Ladders (see **Figure 5.1C** and **Figure 5.1D**), or onto some other neurons (not fully contained in the present EM volume). Particularly, the reduced hunching responses of these animals (see **Figure 5.1J'** and **Figure 5.1K'**) are consistent with the reduced connectivity between Chordotonals and Griddles (see **Figure 5.1C**), since Griddles have been shown to be required for hunching behavior (Jovanic et al., 2016).

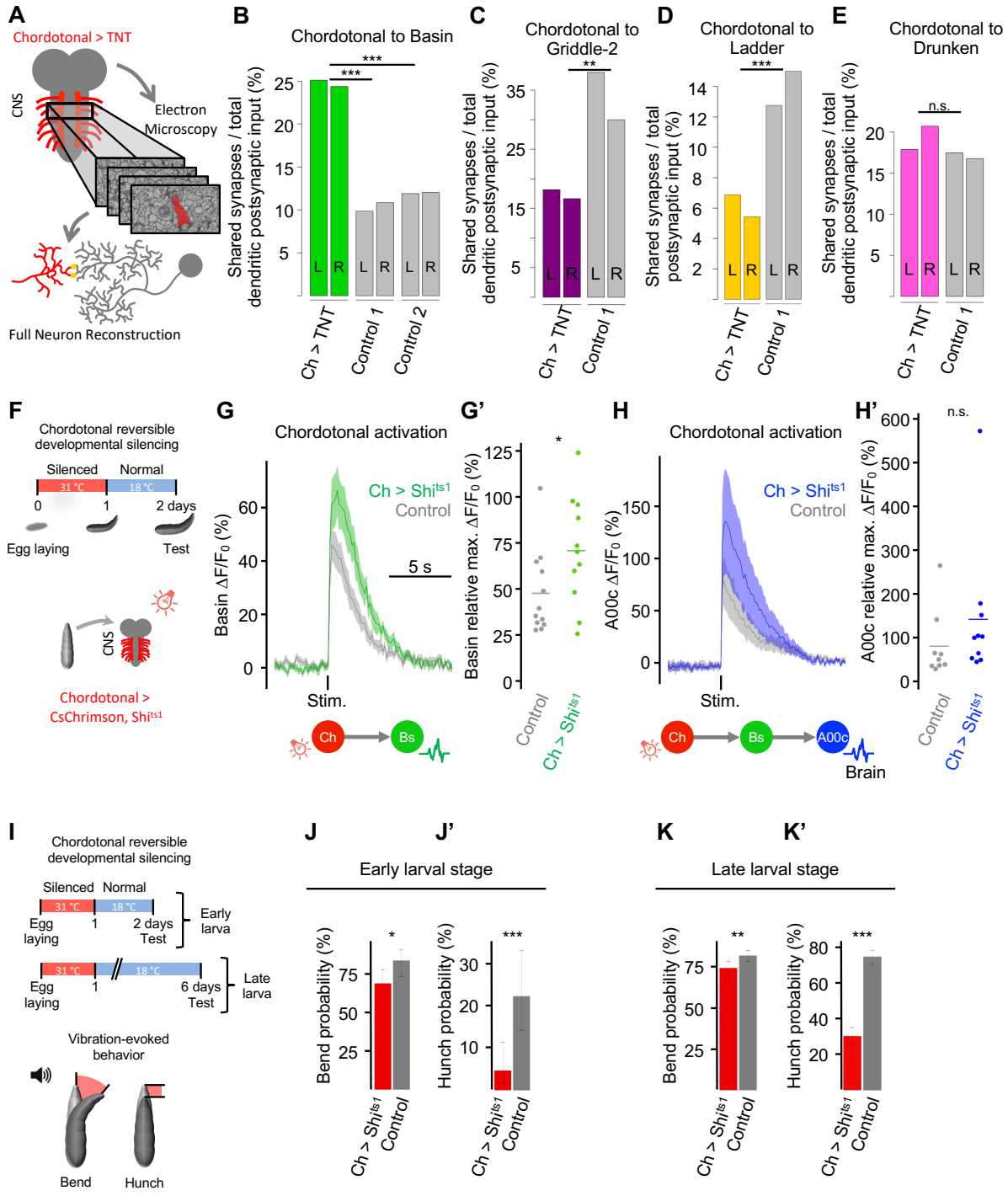

Figure 5.1. Lack of Chordotonal input during development alters the connectivity of the circuit and generates defective behavior.

A) Chordotonal neurons and downstream partners were reconstructed in two different EM volumes: one wildtype (*w1118*) and one in which the Chordotonals were silenced through the expression of TNT (*Ch-*

GAL4 > UAS-TNT). The TNT volume consists of approximately 1.5 abdominal segments. In this volume, the key (i.e. Basin, Ladder, Griddle, and Drunken) Chordotonal partner neurons were fully reconstructed.

B-E) Connectivity revealed by EM reconstructions of Chordotonals (Ch) silenced with TNT and key postsynaptic partners in one abdominal segment of a first instar larva. To report the relative number of connections between partner neurons, the number of synapses from Chordotonals onto the postsynaptic partner was divided by the total number of dendritic (B, C, E) or dendritic and axonal (D) inputs of the postsynaptic partner. The experimental animal's genotype was *w; UAS-TNT/+; Ch-GAL4/+*. Controls were animals of the *w1118* genotype. Connectivity from neurons in the right (R) and left (L) sides is shown separately. However, left and right synapse counts were grouped for statistical analysis.

F) Schematic of the experimental conditions for reversible silencing of Chordotonal neurons during development. Embryos with Chordotonal neurons expressing Shibire^{ts1} (Shi^{ts1}) and CsChrimson were incubated at 31 °C (restrictive temperature) for 24 hours and then transferred to 18 °C (permissive temperature) for another day before testing. Isolated CNS were used to record calcium responses in Basin (G) or A00c (H) to the optogenetic activation of Chordotonal neurons.

G) Basin calcium responses (mean ± s.e.m) to Chordotonal optogenetic activation (Stim., 1040 nm for 100 ms) increase when the Chordotonal neurons were reversibly silenced with Shibire^{ts1} during development (green trace; *Basin-GAL4 > UAS-GCaMP6s, Ch-LexA > LexAop-CsChrimson, LexAop-Shi^{ts1}*; progeny of the cross between fly lines 5 and 7, **Table 1**) compared to control (gray trace; *Basin-GAL4 > UAS-GCaMP6s, Ch-LexA > LexAop-CsChrimson*; progeny of the cross between fly lines 5 and 6, **Table 1**).

G') Quantification of the calcium responses in G. Relative maximum $\Delta F/F_0$ values had the sample-specific baseline subtracted. n= 11 animals for experimental (green); n= 12 animals for control (gray).

H) A00c (a direct downstream partner of Basins) calcium responses (mean ± s.e.m) to the optogenetic activation (Stim., 1040 nm for 200 ms) of Chordotonal cells show a non-statistically-significant increase when Chordotonal cells were silenced during development (blue trace; *A00c-GAL4 > UAS-GCaMP6s, Ch-LexA > LexAop-CsChrimson, LexAop-Shi^{ts1}*; progeny of the cross between fly lines 7 and 8, **Table 1**) compared to control (gray trace; *A00c-GAL4 > UAS-GCaMP6s, Ch-LexA > LexAop-CsChrimson*; progeny of the cross between fly lines 8 and 6, **Table 1**).

H') Quantification of the calcium responses in H. Relative maximum $\Delta F/F_0$ values had the sample-specific baseline subtracted. n= 10 animals for experimental (blue); n= 9 animals for control (gray).

I) Schematic of the experimental conditions for reversible silencing of Chordotonal neurons during development for behavioral experiments. Embryos with Chordotonal neurons expressing Shibire^{ts1} were incubated at 31 °C (restrictive temperature) for 24 hours and then transferred to 18 °C for another day (J-J') or 5 days (K-K') before testing. Animals were stimulated with sound-generated vibration (1000 Hz tone).

J-K') Reversibly silencing Chordotonal cells during development significantly reduces the behavioral responses to vibration of early stage larvae (J-J'), with persisting defects in late stage larvae (K-K'). Larvae in which Chordotonal neurons were silenced during development have lower probability for bending (J, K) and hunching (J', K') responses. Experimental (red) genotype: *Ch-GAL4 > UAS-Shi^{ts1}* (progeny of the cross between fly lines 17 and 31, **Table 1**). Control (gray) genotype: *+ > UAS-Shi^{ts1}* (progeny of the cross between fly lines 31 and 32, **Table 1**). Error bars represent the 95% confidence interval.

J-J') The probabilities for bending and hunching behaviors are lower in early stage larvae in which the Chordotonal neurons were silenced (red) during development than in controls (gray). n= 86 animals for experimental; n= 72 for control.

K, K') The probabilities for bending and hunching behaviors are lower in late stage larvae in which the Chordotonal neurons were silenced (red) during development than in controls (gray). n= 380 animals for experimental; n= 476 for control.

Basin cells compensate for the lack of mechanosensory input by increasing nociceptive input, a separate sensory modality

Basins are multisensory interneurons that receive input from both mechanosensory and nociceptive sensory neurons (Ohyama et al., 2015). I therefore asked whether Basins compensate for the lack of mechanosensory input during development, by increasing input from nociceptive neurons. I looked at the connectivity between Basins and the nociceptive MD IV neurons revealed by EM reconstructions. I found that the fraction of Basin synapses from nociceptive neurons was greater when the Chordotonal neurons were silenced than when they were active (see **Figure 5.2A**).

In order to test whether these additional excitatory connections between nociceptive neurons and Basins are functional, I measured Basin responses to the activation of

nociceptive neurons in animals in which the Chordotonal neurons are permanently silent. I used CsChrimson to activate MD IV neurons with red light, and GCaMP6s to monitor Basin activity. For this purpose, I generated triple-system transgenic fly lines that allowed me to simultaneously target the expression of TNT in Chordotonals (*R61D08-LexA > LexAop-TNT*), CsChrimson in nociceptive MD IV neurons (*ppk-QF2 > QUAS-CsChrimson*), and GCaMP6s in Basins (*R72F11-GAL4 > UAS-GCaMP6s*). This fly line enabled me to measure Basin calcium responses to the optogenetic activation of nociceptive neurons in animals in which the Chordotonal neurons are silenced.

I found that, consistent with the EM connectivity data (see **Figure 5.2A**), Basin cells have significantly greater calcium responses to nociceptive MD IV activation when the Chordotonal neurons were silenced than when they had been active (see **Figure 5.2B and Figure 5.2B'**).

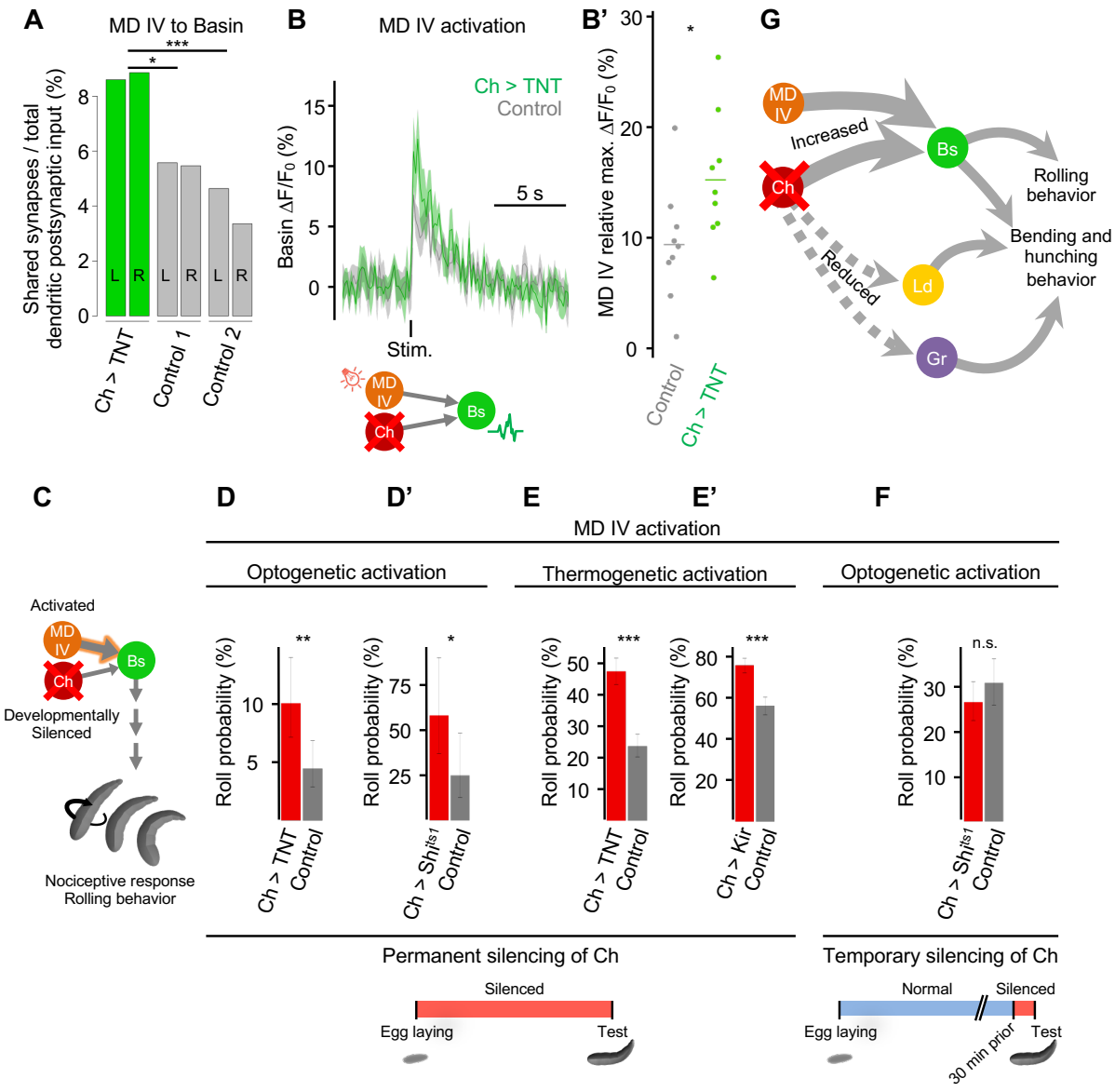

Figure 5.2. Basin cells compensate for the lack of mechanosensory input by increasing their nociceptive input.

A) The fraction of Basin dendritic input that is received from nociceptive MD IV increases when the Chordotonal (Ch) neurons are silenced by the targeted expression of TNT (green bars) as revealed by electron microscopy reconstruction. Controls are two independent *w1118* animals (gray bars). The connectivity from the left (L) and right (R) sides of the nervous system is included to show consistency within sample. Left and right sides were grouped for statistical analysis.

B) Basin calcium responses (mean ± s.e.m.) to the optogenetic activation (Stim., 625 nm for 1 s) of nociceptive MD IV neurons increase when the Chordotonal cells are silenced by the targeted expression of

TNT in third instar larvae (green trace; *Basin-GAL4 > UAS-GCaMP6s, MDIV-QF2 > QUAS-CsChrimson, Ch-LexA > LexAop-TNT*; progeny of the cross between fly lines 9 and 11, **Table 1**). Control responses (gray trace) are from animals lacking the TNT transgene (*Basin-GAL4 > UAS-GCaMP6s, MDIV-QF2 > QUAS-CsChrimson, Ch-LexA > +*; progeny of the cross between fly lines 10 and 11, **Table 1**).

B') Quantification of the calcium responses in B. Relative maximum $\Delta F/F_0$ values had the sample-specific baseline subtracted. n= 9 for each condition.

C) Schematic of the experiment in which Chordotonal neurons were temporarily or permanently silenced, and the MD IV neurons were activated. Since the activation of MD IV normally elicits rolling, this response was used to test for the behavioral effect of the increased connectivity between MD IV and Basins (A) generated by the inactivation of Chordotonals.

D-F) Rolling behavior probabilities of third instar larvae to the activation of nociceptive MD IV neurons and permanent (D-E') or temporary (F) silencing of Chordotonals. Error bars represent 95% confidence interval.

D-E') Optogenetic (D-D') or thermogenetic (E-E') activation of MD IV while Chordotonals were permanently silenced through various methods (TNT for D and E; Shi^{ts1} for D'; Kir for E') led to a higher probability of rolling behavior.

D) Silencing of the Chordotonal neurons with the targeted expression of TNT (red bar; n= 298 animals) produced a higher rolling probability to the optogenetic activation of MD IV compared to control (gray bar; n= 426 animals). Genotypes were the same as in B.

D') Inactivation of Chordotonal neurons expressing Shi^{ts1} and optogenetic activation of MD IV led to increased rolling probability. Animals were incubated at 31 °C for three days, from egg laying until testing. Experimental animals (red) were *Ch-GAL4 > UAS-Shi^{ts1}, MDIV-LexA > LexAop-CsChrimson* (progeny of the cross between fly lines 17 and 14, **Table 1**). Control animals (gray) were *+ > UAS-Shi^{ts1}, MDIV-LexA > LexAop-CsChrimson* (progeny of the cross between fly lines 32 and 14, **Table 1**). Experimental n= 310 animals; control n= 322 animals.

E) Silencing of the Chordotonal neurons with the targeted expression of TNT (red bar; n= 550 animals) produced a higher rolling probability to the thermogenetic activation of MD IV compared to control (gray bar; n= 526 animals). Experimental animals were *MDIV-LexA > LexAop-TrpA1, Ch-GAL4 > UAS-TNT* (progeny of the cross between fly lines 12 and 13, **Table 1**). Control animals were *MDIV-LexA > LexAop-TrpA1, + > UAS-TNT* (progeny of the cross between fly lines 12 and 34, **Table 1**).

E') Silencing of the Chordotonal neurons by the targeted expression of Kir (red bar; n= 580 animals) also led to an increased behavioral response compared to control (gray bar; n= 512 animals). Experimental animals were *MDIV-LexA > LexAop-TrpA1, Ch-GAL4 > UAS-Kir* (progeny of the cross between fly lines 15 and 17, **Table 1**). Control animals were *MD IV-LexA > LexAop-TrpA1, + > UAS-Kir* (progeny of the cross between fly lines 15 and 32, **Table 1**).

F) Temporary silencing of Chordotonal neurons during the experiment (and ≥ 30 minutes before) with Shi^{ts1} has no effect on the rolling probability to the optogenetic activation of MD IV (red bar; n= 399 animals) compared to controls (gray bar; n= 305 animals). This suggests the connectivity compensation observed in A is due to a developmental effect in the circuit and not to the momentary effect of the loss of Chordotonal activity during the experiment. Experimental animals were *Ch-GAL4 > UAS-*Shi^{ts}*, MD IV-LexA > LexAop-CsChrimson* (progeny of the cross between fly lines 14 and 17, **Table 1**). Control animals were *+ > UAS-*Shi^{ts}*, MD IV-LexA > LexAop-CsChrimson* (progeny of the cross between fly lines 14 and 32, **Table 1**).

G) Summary diagram of the connectivity effects of the developmental silencing of Chordotonal neurons. Basin cells (Bs) compensate for the lack of Chordotonal (Ch) input by increasing their input (thick arrow) from inactive (crossed out) Chordotonals. Additionally, Basins also show increased input from a separate sensory modality, the nociceptive multidendritic class IV (MD IV) neurons. This increase in connectivity has an effect on rolling behavior (D-F). However, the inhibitory Ladder (Ld) and Griddle (Gr) neurons lose (dashed arrow) Chordotonal input when Chordotonals were inactive. This decreased connectivity could be responsible for the lower body-bending and hunching behavioral responses observed (see **Figure 5.1J-K'**).

Lack of mechanosensory input results in increased responsiveness to nociceptive stimuli

The experiments described above reveal that Basin neurons increase their nociceptive input to compensate for the lack of Chordotonal input. I therefore asked whether these increased connections have an effect on the behavioral output of the nociceptive circuit. As mentioned before, nociceptive and Basin neurons are part of the circuit underlying the rolling escape response of the larva, and the behavioral responses to their activation have been well characterized (Ohyama et al., 2015). When the animals roll, they bend their bodies into a C shape and spin continuously in a screw-like motion.

I first genetically targeted the expression of TNT in the Chordotonal neurons to silence them constitutively, and CsChrimson in the MD IV neurons for optogenetic activation, just as in **Figure 5.2B**. The rolling behavior probabilities of these animals were significantly greater than those of animals in which the Chordotonals were not silenced (see **Figure 5.2D**). As an alternative approach, I silenced the Chordotonal neurons with Shibire^{ts1} all throughout the animals' lives until testing. These animals also display a significantly greater rolling probability (see **Figure 5.2D'**). These are two analogous experiments that indicate that the developmental silencing of Chordotonal neurons leads to an increased nociceptive sensitivity. To further prove this effect, I decided to use an alternative activation approach by thermogenetically activating the MD IV neurons. I selectively targeted the expression of TrpA1 (Hamada et al., 2008; Kang et al., 2012), a heat-activated cation channel, in the nociceptive MD IV neurons. This allowed me to activate the nociceptive neurons by increasing the temperature of the animals. I thermogenetically activated nociceptive neurons in animals where the Chordotonals had been silenced by the targeted expression of TNT. These animals also displayed significantly greater rolling behavior probabilities than animals in which the Chordotonals were not silenced (see **Figure 5.2E**). In a separate experiment, I silenced the Chordotonal neurons with yet a third effector. I used Kir2.1 (Kir), an inwardly-rectifying potassium channel that hyperpolarizes the neurons and sets the resting membrane potential below the threshold required to fire action potentials (Baines et al., 2001; Johns et al., 1999). This experiment consisted in the thermogenetic activation of nociceptive neurons with TrpA1 and silencing of Chordotonals with Kir. In this case, the activation of nociceptive neurons also evoked significantly stronger rolling responses (see **Figure 5.2DE'**). These four analogous manipulations silenced the Chordotonal neurons (with TNT, Shibire^{ts1} or Kir) and showed the same effect in the behavioral responses to the optogenetic or thermogenetic activation of nociceptive MD IV (see **Figure 5.2D-E'**). These results are consistent with the increased structural and functional connections from nociceptive neurons onto Basins when mechanosensory neurons are silenced (see **Figure 5.2A-B'**).

However, it is unclear whether the increase in these behavioral responses is due to developmental defects in synaptic connectivity that are caused by silencing the Chordotonal neurons, or simply due to the fact that Chordotonals are silenced during the behavioral

experiment (long-term vs short-term effects). Therefore, I tested the effect of Chordotonal inactivation by silencing them exclusively during the experiment, as opposed to silencing them constitutively. In these experiments, the connectivity between Chordotonal neurons and their partners is expected to be as in wildtype since Chordotonal neurons were only inactivated briefly. I therefore optogenetically activated the MD IV neurons with CsChrimson and silenced Chordotonals with Shibire^{ts1} for ≥30 minutes before and during the experiment. I found that experimental and control animals responded to the optogenetic activation of nociceptive neurons with similar rolling probabilities (see **Figure 5.2F**).

Baseline activity of Chordotonal neurons therefore appears to facilitate larval responses to the activation of nociceptive neurons, similar to the previous reports that vibration-mediated activation of Chordotonal neurons facilitates larval rolling response to the activation of nociceptive neurons (Ohyama et al., 2015). Silencing Chordotonals during the experiment had no effect on rolling, while the experiments in which the Chordotonal neurons were permanently silenced with TNT, Shi^{ts1} or Kir had increased rolling responses (see **Figure 5.2D-E'**). Thus, the compensation in connectivity between nociceptive and Basin neurons, calcium responses, and behavior are all likely to be effects of the developmental silencing of the Chordotonal neurons.

Discussion

I examined the effects of silencing the Chordotonal neurons during development on structural and functional connectivity, and behavioral output of the circuit. Connections between silenced Chordotonal neurons and their postsynaptic partners were still present, showing that evoked activity during development does not seem to be required for basic partner recognition. However, the lack of mechanosensory input during development resulted in changes in the strength of connectivity with partner neurons. Additionally, I showed that different elements of the circuit responded differently to the same manipulation, some by increasing their mechanosensory input, and others by reducing it. Interestingly, some Chordotonal partners were also able to compensate for the lack of mechanosensory input by increasing input from a separate sensory modality. I found that animals with constitutively

silenced Chordotonal neurons had reduced behavioral responses to mechanosensory stimuli, and increased responses to nociceptive stimuli, showing that developmental activity is crucial for the normal balance of connections within the circuit.

Similar to my findings, a previous study showed that when motoneurons in the *Drosophila* embryo were silenced with TNT, their morphology and capacity to form synapses were not affected (Baines et al., 2001). Another study showed that rearing animals in complete darkness and depriving them from any visual input had no effect on dendrite or axon complexities of motion sensing neurons in the *Drosophila* visual system (Scott et al., 2003). Similarly, it was shown that evoked or spontaneous activity are not required for the normal wiring of the adult *Drosophila* visual system, as photoreceptors have a normal and constant number of total synapses in various mutants with defective neuronal activity (Hiesinger et al., 2006). They also found this synapse number constancy to be independent of postsynaptic cells, whether they are the correct or incorrect partners. Altogether, these studies show that activity is not required for the normal development of such circuits, consistent particularly with my results in which the silent Chordotonal neurons have normal morphology and connect to their usual partners.

However, I found that the precise fraction of input from the silent Chordotonals onto their postsynaptic partners is changed. Interestingly, the fraction of connections onto some neurons is increased, and decreased onto others, relative to controls.

Connectivity compensation by increasing synapse numbers has been observed previously. Work done in *Drosophila* embryo has shown that motoneurons perform homeostatic regulation of the size of their dendritic arbors based on the amount of presynaptic input (Tripodi et al., 2008). When input onto the motoneurons was blocked by the expression of TNT, the motoneurons responded by increasing the coverage of their dendrites. Another study showed that developing second-order projection neurons in the embryonic antennal lobe of *Drosophila* do not require their presynaptic sensory partners (odor receptor neurons) to be active for survival. However, the lack of input led to slight changes in the postsynaptic arborizations and glomerulus innervations of these neurons (Prieto-Godino et al., 2012). In mice, silenced proprioceptive sensory neurons still contact the appropriate motor targets in

the spinal cord; however, they selectively increased specific connections while others were unchanged (Mendelsohn et al., 2015). These studies show that neurons can change their connections or even morphology in response to the lack of neuronal input.

Increased activity in the circuit during development has also been shown to influence connectivity. Increased visual input, generated by extending periods of light exposure, led to reduced dendritic exploration and arbor length, and premature saturation of the number of synaptic contacts in second-order neurons in the *Drosophila* larva visual system (Sheng et al., 2018; Yuan et al., 2011). Another study also found that developmental stimulation of nociceptive MD IV neurons produced long-lasting suppression of nociceptive behavior in *Drosophila* larva (Kaneko et al., 2017). However, I showed that the lack of Chordotonal input leads to a reduced mechanosensory behavioral response. Similarly, depriving kittens of visual input during an early critical period by suturing their eyelids permanently impaired their vision, even after their eyes were opened again (Hubel and Wiesel, 1964). However, repeatedly depriving adult mice of monocular vision resulted in a shift of neuronal responses to the open eye that was fully reverted every time after regaining vision (Rose et al., 2016). Together with these previous studies, my results suggest that the effects of increasing or abolishing neuronal activity are time-sensitive and may not be simple opposites of each other.

Interestingly, I found that the developmental silencing of Chordotonal neurons leads to connectivity compensation from nociceptive inputs onto multisensory interneurons and increased responsiveness to noxious stimuli. This is similar to the reorganization of the cortex observed in blind cats, in which the visual cortex is invaded by neurons responsive to auditory and somatosensory stimuli (Rauschecker, 1995; Rauschecker and Korte, 1993). Similarly, the auditory cortex of deaf cats reorganizes to process visual stimuli, and is involved in superior visual abilities deaf cats acquired compared to hearing cats (Lomber et al., 2010).

The experiments I described in this chapter differ from previous work in that I combined: 1) the targeted silencing of a defined group of neurons, as opposed to coarse or whole animal manipulations; 2) high-resolution EM reconstruction of the connections between the manipulated neurons and their known specific partners; 3) functional imaging to corroborate modified connections between each pair of partner neurons and; 4) behavioral assays as

evidence of the overall effects of the manipulation on the whole circuit. All of these characteristics combined enabled me to pin down with unprecedented resolution the range of effects of silencing Chordotonal neurons on circuit structure and function.

In summary, I have shown that evoked activity is not required for partner recognition. However, the lack of Chordotonal input during development reshaped the connectivity balance between Chordotonals and their partners. The number of connections from silent Chordotonals onto Bains increased, while the connections onto Ladder and Griddle neurons were reduced. This shows that different elements of the circuit have different abilities to respond to the same manipulation. Interestingly, the multisensory Basin neurons also compensated by increasing their input from a separate sensory modality, the nociceptive MD IV neurons. Animals with Chordotonal neurons that were silenced during development exhibited a range of behavioral defects: both decreased sensitivity to mechanosensory stimuli and increased sensitivity to nociceptive stimuli. These effects are reminiscent of those observed in vertebrates and show that developmental activity is crucial for the normal balance of connections within the insect somatosensory circuit.

General conclusions

In this thesis I have investigated how neural circuits are formed and the developmental rules they use to establish connections. Two prominent theories have been proposed to explain the mechanisms for circuit assembly. First, Peters' rule states that neurons that occupy overlapping areas are more likely to be connected to each other. This suggests location determines partner specificity. Second, Sperry's chemoaffinity theory proposes that neurons express specific molecular tags that allow them to identify and connect to only those neurons carrying the right set of molecular tags. These two seemingly opposite theories were proposed decades ago and the extent to which one or the other is true remained unclear until now.

To test the role of partner location in circuit assembly, I genetically manipulated the Chordotonal neurons to grow in a different location than usual. Surprisingly, I found that their regular postsynaptic partners extended ectopic branches to reach for the displaced Chordotonal neurons. This shows that these neurons must use a partner-specific recognition process that extends partner selectivity beyond locational overlap, supporting Sperry's chemoaffinity theory. Interestingly, the displaced Chordotonal axons preserved most of their top synaptic partners and did not form strong connections with any new neurons at their new location, opposite to what Peters' rule would predict. However, detailed connectivity quantification revealed differences in connectivity strength that indicate the circuit did not wire correctly, despite the morphological and positional compensation from postsynaptic partners. In fact, the mechanosensory behavior of animals with displaced Chordotonal neurons was significantly deficient as a result of these connectivity alterations. This indicates predefined partner location contributes to the amount of connections between partners, but does not determine the identity of the partners involved.

Additionally, I investigated the role of neuronal activity in partner specificity during circuit assembly. I showed that silencing the Chordotonal neurons did not affect the set of top synaptic partners they connect to. However, this developmental silencing changed the strength of connections between them. This connectivity imbalance resulted in long-lasting

behavioral defects that could not be reverted even after restoring activity. Strikingly, upon the lack of mechanosensory input, neurons in the circuit became more sensitive to nociceptive input, a different sensory modality. While developmental activity does not seem to play a role in partner selectivity, it influences the strength of connections between synaptic partners.

Based on these results, I propose the following mechanism for synaptic specificity in circuit assembly. During development, neurons follow predefined trajectories through the nervous system to reach a target location where they will arborize and contact their partners. Once at the target location, they undergo extensive exploration as they sample the available neurons to identify their intended partners. As they explore, neurons use partner-derived cues to identify their partners and stabilize the right contacts to form synapses. However, this exploration is spatially restricted, and the extent of correct partner contacts will depend on this physical exploration range. These connections are then further tuned through activity-dependent mechanisms to optimize the circuit.

EM reconstruction of the mechanosensory Chordotonal circuit revealed detailed connectivity effects with synaptic-resolution of developmental manipulations of the circuit. I performed genetically-targeted manipulations during development of individual elements of the circuit to corroborate the quantified connectivity differences through functional and behavioral experiments. All of these characteristics combined enabled me to dissect the partner selectivity process and reveal the roles of partner location and activity with unprecedented detail.

Altogether, the results presented in this thesis suggest that partner selectivity is a result of a multi-step process in which predefined partner location, partner-specific affinity, and partner activity are all required for normal circuit assembly. This shows Peters' rule and Sperry's chemoaffinity theory are not entirely mutually exclusive but work together to explain circuit formation.

References

Ainsley, J.A., Pettus, J.M., Bosenko, D., Gerstein, C.E., Zinkevich, N., Anderson, M.G., Adams, C.M., Welsh, M.J., and Johnson, W.A. (2003). Enhanced Locomotion Caused by Loss of the Drosophila DEG/ENaC Protein Pickpocket1. Curr. Biol. *13*, 1557–1563.

Araújo, S.J., and Tear, G. (2003). Axon guidance mechanisms and molecules: lessons from invertebrates. Nat. Rev. Neurosci. *4*, 910–922.

Baines, R.A., and Bate, M. (1998). Electrophysiological development of central neurons in the Drosophila embryo. J. Neurosci. *18*, 4673–4683.

Baines, R.A., Uhler, J.P., Thompson, A., Sweeney, S.T., and Bate, M. (2001). Altered electrical properties in Drosophila neurons developing without synaptic transmission. J. Neurosci. *21*, 1523–1531.

Bashaw, G.J., and Goodman, C.S. (1999). Chimeric axon guidance receptors: the cytoplasmic domains of slit and netrin receptors specify attraction versus repulsion. Cell *97*, 917–926.

Berck, M.E., Khandelwal, A., Claus, L., Hernandez-Nunez, L., Si, G., Tabone, C.J., Li, F., Truman, J.W., Fetter, R.D., Louis, M., et al. (2016). The wiring diagram of a glomerular olfactory system. Elife *5*.

Boulanger, J., Kervrann, C., Bouthemy, P., Elbau, P., Sibarita, J.-B., and Salamero, J. (2010). Patch-Based Nonlocal Functional for Denoising Fluorescence Microscopy Image Sequences. IEEE Trans. Med. Imaging *29*, 442–454.

Briggman, K.L., and Bock, D.D. (2012). Volume electron microscopy for neuronal circuit reconstruction. Curr. Opin. Neurobiol. *22*, 154–161.

Brose, K., Bland, K.S., Wang, K.H., Arnott, D., Henzel, W., Goodman, C.S., Tessier-Lavigne, M., and Kidd, T. (1999). Slit proteins bind Robo receptors and have an evolutionarily conserved role in repulsive axon guidance. Cell *96*, 795–806.

Brown, T.H., Zhao, Y., and Leung, V. (2009). Hebbian Plasticity. Encycl. Neurosci. 1049–1056.

Caldwell, J.C., Miller, M.M., Wing, S., Soll, D.R., and Eberl, D.F. (2003). Dynamic analysis of larval locomotion in Drosophila chordotonal organ mutants. Proc. Natl. Acad. Sci. U. S. A. *100*, 16053–16058.

Carrillo, R.A., Olsen, D.P., Yoon, K.S., and Keshishian, H. (2010). Presynaptic Activity and CaMKII Modulate Retrograde Semaphorin Signaling and Synaptic Refinement. Neuron *68*, 32–

44.

Chao, D.L., Ma, L., and Shen, K. (2009). Transient cell–cell interactions in neural circuit formation. Nat. Rev. Neurosci. *10*, 262–271.

Chen, B.E., Kondo, M., Garnier, A., Watson, F.L., Püettmann-Holgado, R., Lamar, D.R., and Schmucker, D. (2006). The molecular diversity of Dscam is functionally required for neuronal wiring specificity in Drosophila. Cell *125*, 607–620.

Chen, M.S., Obar, R.A., Schroeder, C.C., Austin, T.W., Poodry, C.A., Wadsworth, S.C., and Vallee, R.B. (1991). Multiple forms of dynamin are encoded by shibire, a Drosophila gene involved in endocytosis. Nature *351*, 583–586.

Chen, T.-W., Wardill, T.J., Sun, Y., Pulver, S.R., Renninger, S.L., Baohan, A., Schreiter, E.R., Kerr, R.A., Orger, M.B., Jayaraman, V., et al. (2013). Ultrasensitive fluorescent proteins for imaging neuronal activity. Nature *499*, 295–300.

Chilton, J.K. (2006). Molecular mechanisms of axon guidance. Dev. Biol. *292*, 13–24.

Clandinin, T.R., and Zipursky, S.L. (2002). Making Connections in the Fly Visual System. Neuron *35*, 827–841.

Constance, W.D., Mukherjee, A., Fisher, Y.E., Pop, S., Blanc, E., Toyama, Y., and Williams, D.W. (2018). Neurexin and Neuroligin-based adhesion complexes drive axonal arborisation growth independent of synaptic activity. Elife *7*.

Couton, L., Mauss, A.S., Yunusov, T., Diegelmann, S., Evers, J.F., and Landgraf, M. (2015). Development of Connectivity in a Motoneuronal Network in Drosophila Larvae. Curr. Biol. *25*, 568–576.

Denisov, G., Ohyama, T., Jovanic, T., and Zlatic, M. (2013). Model-based Detection and Analysis of Animal Behaviors using Signals Extracted by Automated Tracking. In BIOSIGNALS, p.

Dickson, B.J., and Gilestro, G.F. (2006). Regulation of Commissural Axon Pathfinding by Slit and its Robo Receptors. Annu. Rev. Cell Dev. Biol. *22*, 651–675.

Eichler, K., Li, F., Litwin-Kumar, A., Park, Y., Andrade, I., Schneider-Mizell, C.M., Saumweber, T., Huser, A., Eschbach, C., Gerber, B., et al. (2017). The complete connectome of a learning and memory centre in an insect brain. Nature *548*, 175–182.

Evans, T.A., and Bashaw, G.J. (2010). Functional Diversity of Robo Receptor Immunoglobulin Domains Promotes Distinct Axon Guidance Decisions. Curr. Biol. *20*, 567–572.

Georgiou, M., and Tear, G. (2002). Commissureless is required both in commissural neurones and midline cells for axon guidance across the midline. Development *129*.

Gerhard, S., Andrade, I., Fetter, R.D., Cardona, A., and Schneider-Mizell, C.M. (2017). Conserved neural circuit structure across Drosophila larval development revealed by comparative connectomics. Elife *6*, e29089.

Hamada, F.N., Rosenzweig, M., Kang, K., Pulver, S.R., Ghezzi, A., Jegla, T.J., and Garrity, P.A. (2008). An internal thermal sensor controlling temperature preference in Drosophila. Nature *454*, 217–220.

Harris, R., Sabatelli, L.M., and Seeger, M.A. (1996). Guidance cues at the Drosophila CNS midline: Identification and characterization of two Drosophila Netrin/UNC-6 homologs. Neuron *17*, 217–228.

Hartenstein, V. (1993). Atlas of Drosophila development (Cold Spring Harbor Laboratory Press).

Hebb, D.O. (1949). The Organization of Behavior.

Heiman, M.G., and Shaham, S. (2010). Twigs into branches: how a filopodium becomes a dendrite. Curr. Opin. Neurobiol. *20*, 86–91.

Helmstaedter, M. (2013). Cellular-resolution connectomics: challenges of dense neural circuit reconstruction. Nat. Methods *10*, 501–507.

Helmstaedter, M., Briggman, K.L., and Denk, W. (2011). High-accuracy neurite reconstruction for high-throughput neuroanatomy. Nat. Neurosci. *14*, 1081–1088.

Helmstaedter, M., Briggman, K.L., Turaga, S.C., Jain, V., Seung, H.S., and Denk, W. (2013). Connectomic reconstruction of the inner plexiform layer in the mouse retina. Nature *500*, 168–174.

Hiesinger, P.R., Zhai, R.G., Zhou, Y., Koh, T.W., Mehta, S.Q., Schulze, K.L., Cao, Y., Verstreken, P., Clandinin, T.R., Fischbach, K.F., et al. (2006). Activity-Independent Prespecification of Synaptic Partners in the Visual Map of Drosophila. Curr. Biol. *16*, 1835–1843.

Hong, W., and Luo, L. (2014). Genetic control of wiring specificity in the fly olfactory system. Genetics *196*, 17–29.

Hong, W., Mosca, T.J., and Luo, L. (2012). Teneurins instruct synaptic partner matching in an olfactory map. Nature *484*, 201–207.

Hotta, Y., Hiramoto, M., Hiromi, Y., and Giniger, E. (2000). The Drosophila Netrin receptor Frazzled guides axons by controlling Netrin distribution. Nature *406*, 886–889.

Hubel, D.H., and Wiesel, T.N. (1964). EFFECTS OF MONOCULAR DEPRIVATION IN KITTENS. Naunyn. Schmiedebergs. Arch. Exp. Pathol. Pharmakol. *248*, 492–497.

Hughes, M.E., Bortnick, R., Tsubouchi, A., Bäumer, P., Kondo, M., Uemura, T., and Schmucker, D. (2007). Homophilic Dscam interactions control complex dendrite morphogenesis. Neuron *54*, 417–427.

Hwang, R.Y., Zhong, L., Xu, Y., Johnson, T., Zhang, F., Deisseroth, K., and Tracey, W.D. (2007). Nociceptive Neurons Protect Drosophila Larvae from Parasitoid Wasps. Curr. Biol. *17*, 2105–2116.

Inaki, M., Yoshikawa, S., Thomas, J.B., Aburatani, H., and Nose, A. (2007). Wnt4 is a local repulsive cue that determines synaptic target specificity. Curr. Biol. *17*, 1574–1579.

Jacobs, J.R., and Goodman, C.S. (1989). Embryonic development of axon pathways in the Drosophila CNS. II. Behavior of pioneer growth cones. J. Neurosci. *9*, 2412–2422.

Jarecki, J., and Keshishian, H. (1995). Role of neural activity during synaptogenesis in Drosophila. J. Neurosci. *15*, 8177–8190.

Jefferis, G.S.X.E., Marin, E.C., Stocker, R.F., and Luo, L. (2001). Target neuron prespecification in the olfactory map of Drosophila. Nature *414*, 204–208.

Jefferis, G.S.X.E., Vyas, R.M., Berdnik, D., Ramaekers, A., Stocker, R.F., Tanaka, N.K., Ito, K., and Luo, L. (2004). Developmental origin of wiring specificity in the olfactory system of Drosophila. Development *131*, 117–130.

Jenett, A., Rubin, G.M., Ngo, T.-T.B., Shepherd, D., Murphy, C., Dionne, H., Pfeiffer, B.D., Cavallaro, A., Hall, D., Jeter, J., et al. (2012). A GAL4-Driver Line Resource for Drosophila Neurobiology. Cell Rep. *2*, 991–1001.

Johns, D.C., Marx, R., Mains, R.E., O'Rourke, B., and Marbán, E. (1999). Inducible genetic suppression of neuronal excitability. J. Neurosci. *19*, 1691–1697.

Jovanic, T., Schneider-Mizell, C.M., Shao, M., Masson, J.-B., Denisov, G., Fetter, R.D., Mensh, B.D., Truman, J.W., Cardona, A., and Zlatic, M. (2016). Competitive Disinhibition Mediates Behavioral Choice and Sequences in Drosophila. Cell *167*, 858–870.e19.

Kabra, M., Robie, A.A., Rivera-Alba, M., Branson, S., and Branson, K. (2013). JAABA: interactive machine learning for automatic annotation of animal behavior. Nat. Methods *10*, 64–67.

Kamikouchi, A., Inagaki, H.K., Effertz, T., Hendrich, O., Fiala, A., Göpfert, M.C., and Ito, K. (2009). The neural basis of Drosophila gravity-sensing and hearing. Nature *458*, 165–171.

Kaneko, T., Macara, A.M., Li, R., Hu, Y., Iwasaki, K., Dunnings, Z., Firestone, E., Horvatic, S., Guntur, A., Shafer, O.T., et al. (2017). Serotonergic Modulation Enables Pathway-Specific Plasticity in a Developing Sensory Circuit in Drosophila. Neuron *95*, 623–638.e4.

Kang, K., Panzano, V.C., Chang, E.C., Ni, L., Dainis, A.M., Jenkins, A.M., Regna, K., Muskavitch, M.A.T., and Garrity, P.A. (2012). Modulation of TRPA1 thermal sensitivity enables sensory discrimination in Drosophila. Nature *481*, 76–80.

Kasthuri, N., Hayworth, K.J., Berger, D.R., Schalek, R.L., Conchello, J.A., Knowles-Barley, S., Lee, D., Vázquez-Reina, A., Kaynig, V., Jones, T.R., et al. (2015). Saturated Reconstruction of a Volume of Neocortex. Cell *162*, 648–661.

Katz, L.C., and Shatz, C.J. (1996). Synaptic activity and the construction of cortical circuits. Science *274*, 1133–1138.

Kavlie, R.G., and Albert, J.T. (2013). Chordotonal organs. Curr. Biol. *23*, R334–R335.

Keino-Masu, K., Masu, M., Hinck, L., Leonardo, E.D., Chan, S.S., Culotti, J.G., and Tessier-Lavigne, M. (1996). Deleted in Colorectal Cancer (DCC) encodes a netrin receptor. Cell *87*, 175–185.

Kennedy, T.E., Serafini, T., de la Torre, J.R., and Tessier-Lavigne, M. (1994). Netrins are diffusible chemotropic factors for commissural axons in the embryonic spinal cord. Cell *78*, 425–435.

Kernan, M.J. (2007). Mechanotransduction and auditory transduction in Drosophila. Pflügers Arch. - Eur. J. Physiol. *454*, 703–720.

Keshishian, H., Chiba, A., Chang, T.N., Halfon, M.S., Harkins, E.W., Jarecki, J., Wang, L., Anderson, M., Cash, S., Halpern, M.E., et al. (1993). Cellular mechanisms governing synaptic development inDrosophila melanogaster. J. Neurobiol. *24*, 757–787.

Keshishian, H., Chang, T.N., and Jarecki, J. (1994). Precision and plasticity during Drosophila neuromuscular development. FASEB J. *8*, 731–737.

Kidd, T., Brose, K., Mitchell, K.J., Fetter, R.D., Tessier-Lavigne, M., Goodman, C.S., and Tear, G. (1998a). Roundabout Controls Axon Crossing of the CNS Midline and Defines a Novel Subfamily of Evolutionarily Conserved Guidance Receptors. Cell *92*, 205–215.

Kidd, T., Russell, C., Goodman, C.S., and Tear, G. (1998b). Dosage-Sensitive and

Complementary Functions of Roundabout and Commissureless Control Axon Crossing of the CNS Midline. Neuron *20*, 25–33.

Kidd, T., Bland, K.S., and Goodman, C.S. (1999). Slit is the midline repellent for the robo receptor in Drosophila. Cell *96*, 785–794.

Kitamoto, T. (2001). Conditional modification of behavior inDrosophila by targeted expression of a temperature-sensitiveshibire allele in defined neurons. J. Neurobiol. *47*, 81–92.

Klapoetke, N.C., Murata, Y., Kim, S.S., Pulver, S.R., Birdsey-Benson, A., Cho, Y.K., Morimoto, T.K., Chuong, A.S., Carpenter, E.J., Tian, Z., et al. (2014). Independent optical excitation of distinct neural populations. Nat. Methods *11*, 338–346.

Koch, D., Rosoff, W.J., Jiang, J., Geller, H.M., and Urbach, J.S. (2012). Strength in the Periphery: Growth Cone Biomechanics and Substrate Rigidity Response in Peripheral and Central Nervous System Neurons. Biophys. J. *102*, 452–460.

Kohsaka, H., and Nose, A. (2009). Target recognition at the tips of postsynaptic filopodia: accumulation and function of Capricious. Development *136*, 1127–1135.

Kolodziej, P.A., Timpe, L.C., Mitchell, K.J., Fried, S.R., Goodman, C.S., Jan, L.Y., and Jan, Y.N. (1996). frazzled Encodes a Drosophila Member of the DCC Immunoglobulin Subfamily and Is Required for CNS and Motor Axon Guidance. Cell *87*, 197–204.

Koser, D.E., Thompson, A.J., Foster, S.K., Dwivedy, A., Pillai, E.K., Sheridan, G.K., Svoboda, H., Viana, M., Costa, L. da F., Guck, J., et al. (2016). Mechanosensing is critical for axon growth in the developing brain. Nat. Neurosci. *19*, 1592–1598.

Kwon, Y., Shen, W.L., Shim, H.-S., and Montell, C. (2010). Fine thermotactic discrimination between the optimal and slightly cooler temperatures via a TRPV channel in chordotonal neurons. J. Neurosci. *30*, 10465–10471.

Le, T., Liang, Z., Patel, H., Yu, M.H., Sivasubramaniam, G., Slovitt, M., Tanentzapf, G., Mohanty, N., Paul, S.M., Wu, V.M., et al. (2006). A New Family of Drosophila Balancer Chromosomes With a w- dfd-GMR Yellow Fluorescent Protein Marker. Genet. Soc. Am.

Lee, W.-C.A., Bonin, V., Reed, M., Graham, B.J., Hood, G., Glattfelder, K., and Reid, R.C. (2016). Anatomy and function of an excitatory network in the visual cortex. Nature *532*, 370–374.

Leighton, A.H., and Lohmann, C. (2016). The Wiring of Developing Sensory Circuits—From Patterned Spontaneous Activity to Synaptic Plasticity Mechanisms. Front. Neural Circuits *10*, 71.

Li, H., Shuster, S.A., Li, J., and Luo, L. (2018). Linking neuronal lineage and wiring specificity. Neural Dev. *13*, 5.

Li, W.-C., Cooke, T., Sautois, B., Soffe, S.R., Borisyuk, R., and Roberts, A. (2007). Axon and dendrite geography predict the specificity of synaptic connections in a functioning spinal cord network. Neural Dev. *2*, 17.

Lohmann, C., and Bonhoeffer, T. (2008). A Role for Local Calcium Signaling in Rapid Synaptic Partner Selection by Dendritic Filopodia. Neuron *59*, 253–260.

Lohmann, C., Myhr, K.L., and Wong, R.O.L. (2002). Transmitter-evoked local calcium release stabilizes developing dendrites. Nature *418*, 177–181.

Lomber, S.G., Meredith, M.A., and Kral, A. (2010). Cross-modal plasticity in specific auditory cortices underlies visual compensations in the deaf. Nat. Neurosci. *13*, 1421–1427.

Long, H., Sabatier, C., Ma, L., Plump, A., Yuan, W., Ornitz, D.M., Tamada, A., Murakami, F., Goodman, C.S., and Tessier-Lavigne, M. (2004). Conserved roles for Slit and Robo proteins in midline commissural axon guidance. Neuron *42*, 213–223.

Matthews, B.J., Kim, M.E., Flanagan, J.J., Hattori, D., Clemens, J.C., Zipursky, S.L., and Grueber, W.B. (2007). Dendrite self-avoidance is controlled by Dscam. Cell *129*, 593–604.

Mendelsohn, A.I., Simon, C.M., Abbott, L.F., Mentis, G.Z., and Jessell, T.M. (2015). Activity Regulates the Incidence of Heteronymous Sensory-Motor Connections. Neuron *87*, 111–123.

Menon, K.P., Carrillo, R.A., and Zinn, K. (2013). Development and plasticity of the Drosophila larval neuromuscular junction. Wiley Interdiscip. Rev. Dev. Biol. *2*, 647–670.

Merritt, D.J., and Whitington, P.M. (1995). Central projections of sensory neurons in the Drosophila embryo correlate with sensory modality, soma position, and proneural gene function. J. Neurosci. *15*, 1755–1767.

Meyer, R.L. (1998). Roger Sperry and his chemoaffinity hypothesis. Neuropsychologia *36*, 957–980.

Millard, S.S., and Pecot, M.Y. (2018). Strategies for assembling columns and layers in the Drosophila visual system. Neural Dev. *13*, 11.

Millard, S.S., Lu, Z., Zipursky, S.L., and Meinertzhagen, I.A. (2010). Drosophila dscam proteins regulate postsynaptic specificity at multiple-contact synapses. Neuron *67*, 761–768.

Mitchell, J., Maguire, J., and Davenport, A. (2009). Emerging pharmacology and physiology of

neuromedin U and the structurally related peptide neuromedin S. Br. J. Pharmacol. *158*, 87–103.

Mogami, K., and Hotta, Y. (1981). Isolation of Drosophila flightless mutants which affect myofibrillar proteins of indirect flight muscle. Mol. Gen. Genet. *183*, 409–417.

Nériec, N., and Desplan, C. (2016). From the Eye to the Brain: Development of the Drosophila Visual System. Curr. Top. Dev. Biol. *116*, 247–271.

O'Donnell, P.T., and Bernstein, S.I. (1988). Molecular and ultrastructural defects in a Drosophila myosin heavy chain mutant: differential effects on muscle function produced by similar thick filament abnormalities. J. Cell Biol. *107*, 2601–2612.

Ohyama, T., Jovanic, T., Denisov, G., Dang, T.C., Hoffmann, D., Kerr, R.A., and Zlatic, M. (2013). High-Throughput Analysis of Stimulus-Evoked Behaviors in Drosophila Larva Reveals Multiple Modality-Specific Escape Strategies. PLoS One *8*, e71706.

Ohyama, T., Schneider-Mizell, C.M., Fetter, R.D., Valdes-Aleman, J., Franconville, R., Rivera-Alba, M., Mensh, B.D., Branson, K.M., Simpson, J.H., Truman, J.W., et al. (2015). A multilevel multimodal circuit enhances action selection in Drosophila. Nature *520*, 633–639.

Pasterkamp, R.J., and Kolodkin, A.L. (2003). Semaphorin junction: making tracks toward neural connectivity. Curr. Opin. Neurobiol. *13*, 79–89.

Peters, A., and Feldman, M.L. (1976). The projection of the lateral geniculate nucleus to area 17 of the rat cerebral cortex. I. General description. J. Neurocytol. *5*, 63–84.

Pfeiffer, B.D., Jenett, A., Hammonds, A.S., Ngo, T.-T.B., Misra, S., Murphy, C., Scully, A., Carlson, J.W., Wan, K.H., Laverty, T.R., et al. (2008). Tools for neuroanatomy and neurogenetics in Drosophila. Proc. Natl. Acad. Sci. *105*, 9715–9720.

Pfeiffer, B.D., Ngo, T.-T.B., Hibbard, K.L., Murphy, C., Jenett, A., Truman, J.W., and Rubin, G.M. (2010). Refinement of Tools for Targeted Gene Expression in Drosophila. Genetics *186*, 735–755.

Prieto-Godino, L.L., Diegelmann, S., and Bate, M. (2012). Embryonic Origin of Olfactory Circuitry in Drosophila: Contact and Activity-Mediated Interactions Pattern Connectivity in the Antennal Lobe. PLoS Biol. *10*, e1001400.

R Core Team (2015). R: A Language and Environment for Statistical Computing.

Rajagopalan, S., Vivancos, V., Nicolas, E., and Dickson, B.J. (2000). Selecting a longitudinal pathway: Robo receptors specify the lateral position of axons in the Drosophila CNS. Cell *103*,

1033–1045.

Rauschecker, J.P. (1995). Compensatory plasticity and sensory substitution in the cerebral cortex. Trends Neurosci. *18*, 36–43.

Rauschecker, J.P., and Korte, M. (1993). Auditory compensation for early blindness in cat cerebral cortex. J. Neurosci. *13*, 4538–4548.

Rawson, R.L., Martin, E.A., and Williams, M.E. (2017). Mechanisms of input and output synaptic specificity: finding partners, building synapses, and fine-tuning communication. Curr. Opin. Neurobiol. *45*, 39–44.

Rees, C.L., Moradi, K., and Ascoli, G.A. (2017). Weighing the Evidence in Peters' Rule: Does Neuronal Morphology Predict Connectivity? Trends Neurosci. *40*, 63–71.

Roberts, A., Conte, D., Hull, M., Merrison-Hort, R., al Azad, A.K., Buhl, E., Borisyuk, R., and Soffe, S.R. (2014). Can simple rules control development of a pioneer vertebrate neuronal network generating behavior? J. Neurosci. *34*, 608–621.

Robertson, J.L., Tsubouchi, A., and Tracey, W.D. (2013). Larval Defense against Attack from Parasitoid Wasps Requires Nociceptive Neurons. PLoS One *8*, e78704.

Rose, T., Jaepel, J., Hübener, M., and Bonhoeffer, T. (2016). Cell-specific restoration of stimulus preference after monocular deprivation in the visual cortex. Science *352*, 1319–1322.

Rueden, C.T., Schindelin, J., Hiner, M.C., DeZonia, B.E., Walter, A.E., Arena, E.T., and Eliceiri, K.W. (2017). ImageJ2: ImageJ for the next generation of scientific image data. BMC Bioinformatics *18*, 529.

Saalfeld, S., Cardona, A., Hartenstein, V., and Tomancak, P. (2009). CATMAID: collaborative annotation toolkit for massive amounts of image data. Bioinformatics *25*, 1984–1986.

Schindelin, J., Arganda-Carreras, I., Frise, E., Kaynig, V., Longair, M., Pietzsch, T., Preibisch, S., Rueden, C., Saalfeld, S., Schmid, B., et al. (2012). Fiji: an open-source platform for biological-image analysis. Nat. Methods *9*, 676–682.

Schlegel, P., Texada, M.J., Miroschnikow, A., Schoofs, A., Hückesfeld, S., Peters, M., Schneider-Mizell, C.M., Lacin, H., Li, F., Fetter, R.D., et al. (2016). Synaptic transmission parallels neuromodulation in a central food-intake circuit. Elife *5*.

Schmucker, D., Clemens, J.C., Shu, H., Worby, C.A., Xiao, J., Muda, M., Dixon, J.E., and Zipursky, S.L. (2000). Drosophila Dscam Is an Axon Guidance Receptor Exhibiting Extraordinary

Molecular Diversity. Cell *101*, 671–684.

Schneider-Mizell, C.M., Gerhard, S., Longair, M., Kazimiers, T., Li, F., Zwart, M.F., Champion, A., Midgley, F.M., Fetter, R.D., Saalfeld, S., et al. (2016). Quantitative neuroanatomy for connectomics in Drosophila. Elife *5*.

Schrader, S., and Merritt, D.J. (2000). Central projections of Drosophila sensory neurons in the transition from embryo to larva. J. Comp. Neurol. *425*, 34–44.

Schwabe, T., Borycz, J.A., Meinertzhagen, I.A., and Clandinin, T.R. (2014). Differential adhesion determines the organization of synaptic fascicles in the Drosophila visual system. Curr. Biol. *24*, 1304–1313.

Scott, E.K., Reuter, J.E., and Luo, L. (2003). Dendritic development of Drosophila high order visual system neurons is independent of sensory experience. BMC Neurosci. *4*, 14.

Serafini, T., Kennedy, T.E., Galko, M.J., Mirzayan, C., Jessell, T.M., and Tessier-Lavigne, M. (1994). The netrins define a family of axon outgrowth-promoting proteins homologous to C. elegans UNC-6. Cell *78*, 409–424.

Shanbhag, S.R., Singh, K., and Naresh Singh, R. (1992). Ultrastructure of the femoral chordotonal organs and their novel synaptic organization in the legs of Drosophila melanogaster Meigen (Diptera : Drosophilidae). Int. J. Insect Morphol. Embryol. *21*, 311–322.

Shen, K., and Scheiffele, P. (2010). Genetics and Cell Biology of Building Specific Synaptic Connectivity. Annu. Rev. Neurosci. *33*, 473–507.

Sheng, C., Javed, U., Gibbs, M., Long, C., Yin, J., Qin, B., and Yuan, Q. (2018). Experience-dependent structural plasticity targets dynamic filopodia in regulating dendrite maturation and synaptogenesis. Nat. Commun. *9*, 3362.

Simpson, J.H., Bland, K.S., Fetter, R.D., and Goodman, C.S. (2000a). Short-Range and Long-Range Guidance by Slit and Its Robo Receptors: A Combinatorial Code of Robo Receptors Controls Lateral Position. Cell *103*, 1019–1032.

Simpson, J.H., Kidd, T., Bland, K.S., and Goodman, C.S. (2000b). Short-Range and Long-Range Guidance by Slit and Its Robo Receptors: Robo and Robo2 Play Distinct Roles in Midline Guidance. Neuron *28*, 753–766.

Soba, P., Zhu, S., Emoto, K., Younger, S., Yang, S.-J., Yu, H.-H., Lee, T., Jan, L.Y., and Jan, Y.-N. (2007). Drosophila Sensory Neurons Require Dscam for Dendritic Self-Avoidance and Proper Dendritic Field Organization. Neuron *54*, 403–416.

Sommer, C., Straehle, C., Koethe, U., and Hamprecht, F.A. (2011). ilastik: Interactive Learning and Segmentation Toolkit. In 8th IEEE International Symposium on Biomedical Imaging (ISBI 2011), p.

Sperry, R.W. (1943). Effect of 180 degree rotation of the retinal field on visuomotor coordination. J. Exp. Zool. *92*, 263–279.

Sperry, R.W. (1963). CHEMOAFFINITY IN THE ORDERLY GROWTH OF NERVE FIBER PATTERNS AND CONNECTIONS. Proc. Natl. Acad. Sci. *50*, 703–710.

Sugie, A., Marchetti, G., and Tavosanis, G. (2018). Structural aspects of plasticity in the nervous system of Drosophila. Neural Dev. *13*, 14.

Sürmeli, G., Akay, T., Ippolito, G.C., Tucker, P.W., and Jessell, T.M. (2011). Patterns of spinal sensory-motor connectivity prescribed by a dorsoventral positional template. Cell *147*, 653–665.

Sweeney, S.T., Broadie, K., Keane, J., Niemann, H., and O'Kane, C.J. (1995). Targeted expression of tetanus toxin light chain in Drosophila specifically eliminates synaptic transmission and causes behavioral defects. Neuron *14*, 341–351.

Takemura, S., Bharioke, A., Lu, Z., Nern, A., Vitaladevuni, S., Rivlin, P.K., Katz, W.T., Olbris, D.J., Plaza, S.M., Winston, P., et al. (2013). A visual motion detection circuit suggested by Drosophila connectomics. Nature *500*, 175–181.

Takemura, S., Xu, C.S., Lu, Z., Rivlin, P.K., Parag, T., Olbris, D.J., Plaza, S., Zhao, T., Katz, W.T., Umayam, L., et al. (2015). Synaptic circuits and their variations within different columns in the visual system of Drosophila. Proc. Natl. Acad. Sci. U. S. A. *112*, 13711–13716.

Tavosanis, G. (2012). Dendritic structural plasticity. Dev. Neurobiol. *72*, 73–86.

Tear, G., Harris, R., Sutaria, S., Kilomanski, K., Goodman, C.S., and Seeger, M.A. (1996). commissureless Controls Growth Cone Guidance across the CNS Midline in Drosophila and Encodes a Novel Membrane Protein. Neuron *16*, 501–514.

Tessier-Lavigne, M., and Goodman, C.S. (1996). The molecular biology of axon guidance. Science *274*, 1123–1133.

Timofeev, K., Joly, W., Hadjieconomou, D., and Salecker, I. (2012). Localized Netrins Act as Positional Cues to Control Layer-Specific Targeting of Photoreceptor Axons in Drosophila. Neuron *75*, 80–93.

Tracey, W.D., Wilson, R.I., Laurent, G., and Benzer, S. (2003). painless, a Drosophila Gene

Essential for Nociception. Cell *113*, 261–273.

Tripodi, M., Evers, J.F., Mauss, A., Bate, M., and Landgraf, M. (2008). Structural Homeostasis: Compensatory Adjustments of Dendritic Arbor Geometry in Response to Variations of Synaptic Input. PLoS Biol. *6*, e260.

Utashiro, N., Williams, C.R., Parrish, J.Z., and Emoto, K. (2018). Prior activity of olfactory receptor neurons is required for proper sensory processing and behavior in Drosophila larvae. Sci. Rep. *8*, 8580.

del Valle Rodríguez, A., Didiano, D., and Desplan, C. (2012). Power tools for gene expression and clonal analysis in Drosophila. Nat. Methods *9*, 47–55.

Venken, K.J.T., Simpson, J.H., and Bellen, H.J. (2011). Genetic Manipulation of Genes and Cells in the Nervous System of the Fruit Fly. Neuron *72*, 202–230.

Vogelstein, J.T., Park, Y., Ohyama, T., Kerr, R.A., Truman, J.W., Priebe, C.E., and Zlatic, M. (2014). Discovery of brainwide neural-behavioral maps via multiscale unsupervised structure learning. Science *344*, 386–392.

Vonhoff, F., and Keshishian, H. (2017a). Activity-Dependent Synaptic Refinement: New Insights from Drosophila. Front. Syst. Neurosci. *11*, 23.

Vonhoff, F., and Keshishian, H. (2017b). In Vivo Calcium Signaling during Synaptic Refinement at the Drosophila Neuromuscular Junction. J. Neurosci. *37*, 5511–5526.

White, J.G., Southgate, E., Thomson, J.N., and Brenner, S. (1986). The structure of the nervous system of the nematode Caenorhabditis elegans. Philos. Trans. R. Soc. Lond. B. Biol. Sci. *314*, 1–340.

Wickham, H. (2009). ggplot2: Elegant Graphics for Data Analysis (New York: Springer-Verlag).

Williams, M.E., de Wit, J., and Ghosh, A. (2010). Molecular mechanisms of synaptic specificity in developing neural circuits. Neuron *68*, 9–18.

Wu, Z., Sweeney, L.B., Ayoob, J.C., Chak, K., Andreone, B.J., Ohyama, T., Kerr, R., Luo, L., Zlatic, M., and Kolodkin, A.L. (2011). A Combinatorial Semaphorin Code Instructs the Initial Steps of Sensory Circuit Assembly in the Drosophila CNS. Neuron *70*, 281–298.

Yuan, Q., Xiang, Y., Yan, Z., Han, C., Jan, L.Y., and Jan, Y.N. (2011). Light-induced structural and functional plasticity in Drosophila larval visual system. Science *333*, 1458–1462.

Zheng, Z., Lauritzen, J.S., Perlman, E., Robinson, C.G., Nichols, M., Milkie, D., Torrens, O., Price,

J., Fisher, C.B., Sharifi, N., et al. (2018). A Complete Electron Microscopy Volume of the Brain of Adult Drosophila melanogaster. Cell *174*, 730–743.e22.

Zhu, H., Hummel, T., Clemens, J.C., Berdnik, D., Zipursky, S.L., and Luo, L. (2006). Dendritic patterning by Dscam and synaptic partner matching in the Drosophila antennal lobe. Nat. Neurosci. *9*, 349–355.

Zipursky, S.L., and Grueber, W.B. (2013). The Molecular Basis of Self-Avoidance. Annu. Rev. Neurosci. *36*, 547–568.

Zito, K., Parnas, D., Fetter, R.D., Isacoff, E.Y., and Goodman, C.S. (1999). Watching a Synapse Grow: Noninvasive Confocal Imaging of Synaptic Growth in Drosophila. Neuron *22*, 719–729.

Zlatic, M., Landgraf, M., and Bate, M. (2003). Genetic Specification of Axonal Arbors: atonal Regulates robo3 to Position Terminal Branches in the Drosophila Nervous System. Neuron *37*, 41–51.

Zlatic, M., Li, F., Strigini, M., Grueber, W., and Bate, M. (2009). Positional Cues in the Drosophila Nerve Cord: Semaphorins Pattern the Dorso-Ventral Axis. PLoS Biol. *7*, e1000135.

Supplemental figures

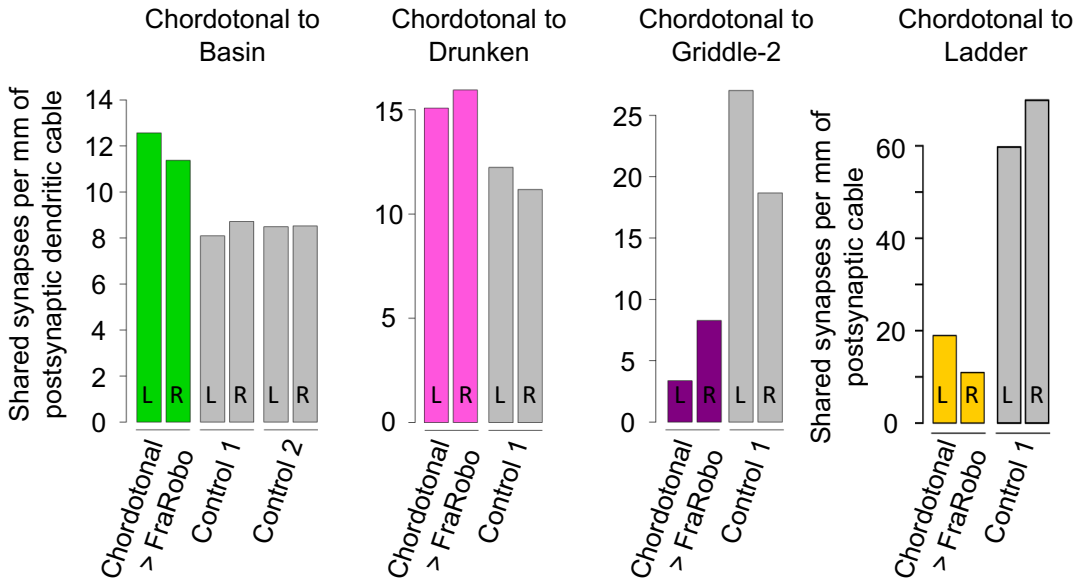

Figure S1. Connectivity between Chordotonal and key postsynaptic partners in a Chordotonal>FraRobo EM volume normalized by cable length.

Connectivity between FraRobo-expressing Chordotonal neurons and key postsynaptic partners is altered. The number of synapses from Chordotonals onto the dendrites of the postsynaptic partner was divided by the cable length of dendritic or total postsynaptic arbor. Connectivity from neurons in the right (R) and left (L) sides of one segment is shown separately. These effects are the same as shown in **Figure 4.4E-H**.

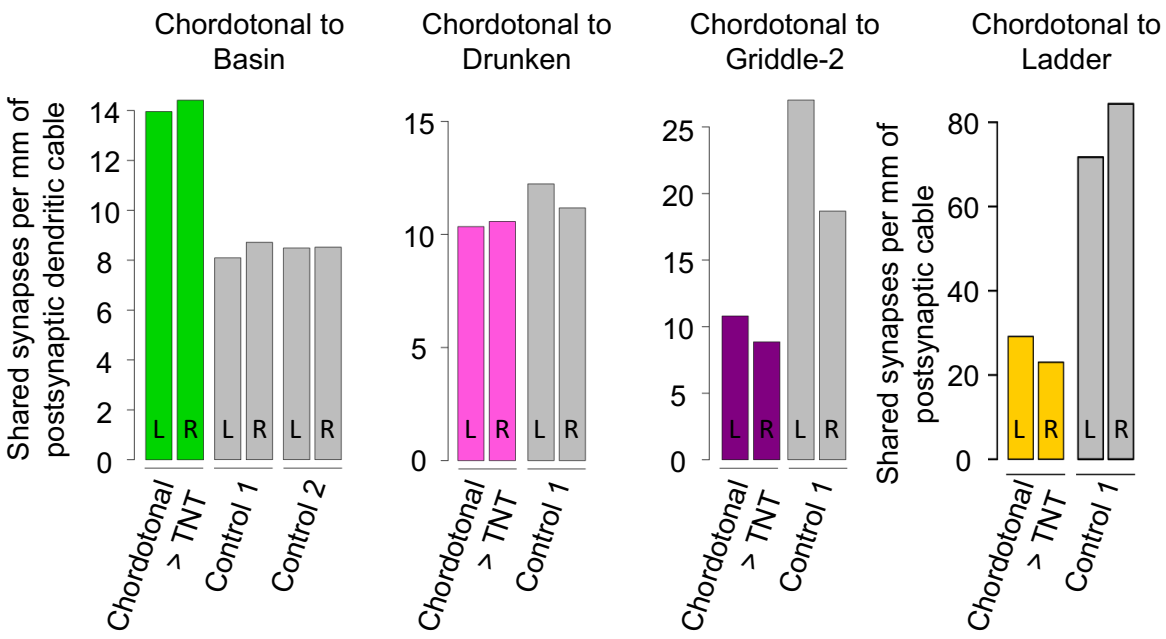

Figure S2. Connectivity between Chordotonal and key postsynaptic partners in a Chordotonal>TNT EM volume normalized by cable length.

Connectivity between silenced Chordotonal neurons and key postsynaptic partners is altered. The number of synapses from Chordotonals onto the dendrites of the postsynaptic partner was divided by the cable length of dendritic or total postsynaptic arbor. Connectivity from neurons in the right (R) and left (L) sides of one segment is shown separately. These effects are the same as shown in **Figure 5.1B-E**.

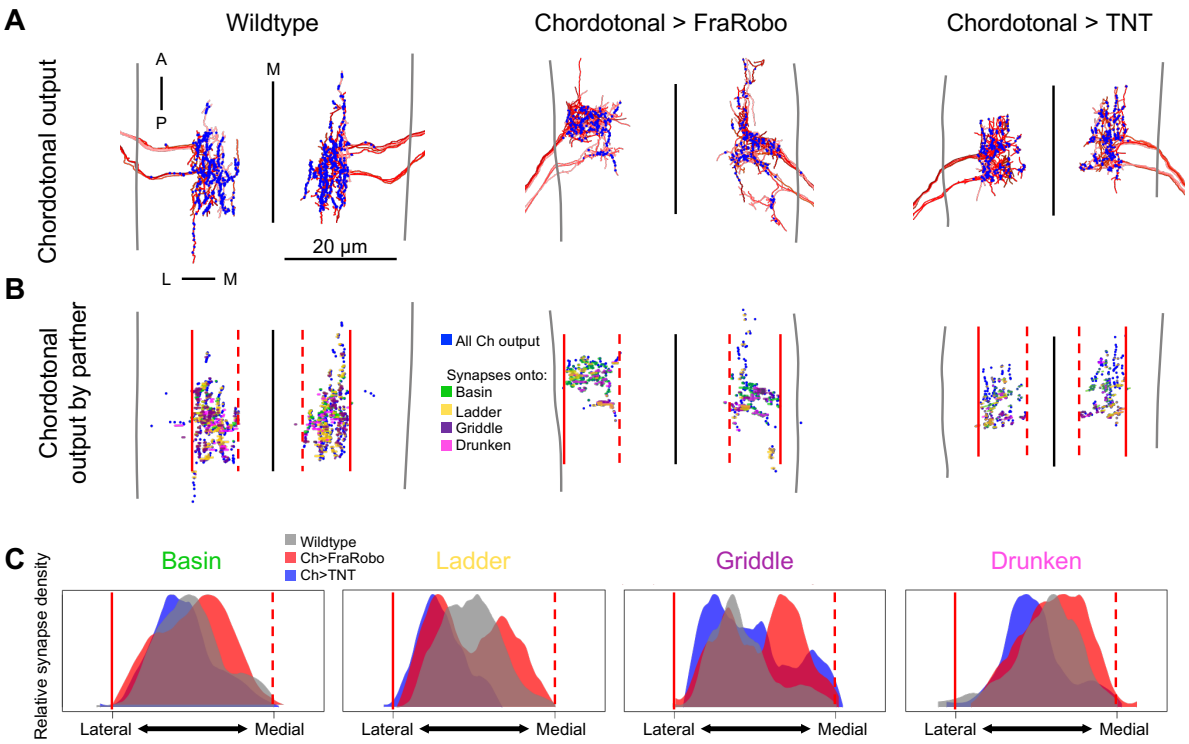

Figure S3. Chordotonal synaptic distribution by partner in wildtype, Chordotonal>FraRobo and Chordotonal>TNT.

A) All presynaptic sites (blue) of Chordotonal axons (red) in one abdominal segment reveled by EM reconstruction. Gray vertical lines indicate the edge of the neuropil. Black line indicates the midline.

B) All Chordotonal (Ch) partner postsynaptic sites color-coded by partner. Red lines indicate the lateral (solid) and medial (dashed) edges of the bulk of Chordotonal presynaptic sites.

C) Synaptic density distribution in the mediolateral axis by partner. Left and right sides were combined in these distributions. Red lines (solid and dashed) represent the same mediolateral locations as in B.